Hindawi
Mathematical Problems in Engineering
Volume 2022, Article ID 5104350, 21 pages
https://doi.org/10.1155/2022/5104350

Research Article

Fractional Conformable Stochastic Integrodifferential Equations: Existence, Uniqueness, and Numerical Simulations Utilizing the Shifted Legendre Spectral Collocation Algorithm

Haneen Badawi,[1] Nabil Shawagfeh,[1] and Omar Abu Arqub [2]

[1]*Department of Mathematics, Faculty of Science, The University of Jordan, Amman 11942, Jordan*
[2]*Department of Mathematics, Faculty of Science, Al-Balqa Applied University, Salt 19117, Jordan*

Correspondence should be addressed to Omar Abu Arqub; o.abuarqub@bau.edu.jo

Received 8 September 2022; Accepted 31 October 2022; Published 28 November 2022

Academic Editor: Kazem Nouri

Theoretical and numerical studies of fractional conformable stochastic integrodifferential equations are introduced in this study. Herein, to emphasize the solution's existence, we provide proof based on Picard iterations and Arzela−Ascoli's theorem, whilst the proof of the uniqueness mainly depends on the famous Gronwall's inequality. Also, we introduce the basic concepts related to shifted Legendre orthogonal polynomials which are utilized to be the basic functions of the spectral collocation algorithm to obtain approximate solutions for the mentioned equations that are not easy to be solved analytically. The substantial idea of the proposed algorithm is to transform such equations into a system containing a finite number of algebraic equations that can be treated using familiar numerical methods. For computational aims, we make a suitable discretization to evaluate the values of the Brownian motion, the noise term considered in our problem, at specific points. In addition, the feasibility and efficiency of the proposed algorithm are proved through convergence analysis and mathematical examples. To exhibit the mathematical simulation, graphs and tables are lucidly shown. Obviously, the physical interpretation of the displayed graphics accurately describes the behavior of the solutions. Despite the simplicity of the presented technique, it produces accurate and reasonable results as notarized in the conclusion section.

1. Introduction

Recently, greater growth of fractional calculus has been developed by many researchers. Since several real-world phenomena in assorted fields of science are represented successfully via models involving fractional derivatives, mathematicians have focused their attention on doing their best to make deeper studies that improve this branch of calculus and its properties. The mathematicians constructed a variety of definitions of fractional derivative operators with their associated integral inverses together with several important related theories. For example, Hadamard [1] suggested a new approach to fractional derivatives, Khalil et al. [2] constructed the CFD and presented some related theories, Caputo and Fabrizio [3] developed a fractional derivative definition that avoids singularity, and Atangana and Baleanu [4] provided the fractional ABC derivative and discussed its properties. In this regard, authors have employed fractional models for various problems. Ahmed et al. [5] built a fractional-order model to describe cancer with two immune effectors. Rihan [6] was concerned with modeling biological systems in fractional models. Xu [7] constructed a fractional model of the Volterra type of population growth. Debnath [8] sheds light on fractional calculus applications concerning engineering and science with numerical solutions to fractional problems of particular types. The well-posedness and the simulated solutions of the FDEs occupy a great status in applied analysis and engineering applications. For complicated problems that have no exact analytic solutions, various operative numerical

techniques have been proposed and employed to provide approximate numerical solutions. Mainly, variational iteration [9], differential transform [10], spectral collocation algorithm [11], finite difference approach [12], and Laplace resolvent kernel scheme [13] are the most popular used methods.

More recently, it is noticed that fractional SDEs are more adapted to natural real-world phenomena than deterministic ones. Specifically, the fractional SDEs are FDEs in which one or more of its terms are stochastic processes. These equations have been used to model natural systems in which the past affects the present and future as mechanical systems, population growth, and financial markets. In the last few years, various problems in biology, anthropology, economics, medical models, finance, and engineering have been modeled in terms of fractional SDEs. Dung [14] studied the quasi-linear SDEs driven by fractional SBM and its application to finance. Lima [15] employed a fractional SDE model to utilize COVID-19. Han et al. [16] discussed SDEs of fractional SBM where the stochastic integral is of Stieltjes type. Pei et al. [17] established an averaging principle to deal with SDEs with fractional SBM where the stochastic integral is of Itô's type. The first issue in solving such equations is to guarantee the presence and assert the exclusivity of their suggested solutions under suitable assumptions. This has been the objective of several studies done by many mathematicians. Guo et al. [18] introduced fractional SDEs in the Caputo sense and provided the existence and uniqueness study of its solution with Caratheodory's approximation for the considered equation. Zhan et al. [19] studied the existence of mild solution, under suitable conditions, for fractional SDEs where the initial conditions are nonlocal. Moualkia and Xu [20] utilized the Picard iterations' theory to emphasize the existence and uniqueness of nonlinear fractional $k - D$ of SDEs with Caputo derivative of variable order. Zheng et al. [21] proved the well-posedness of fractional SDEs with stochastic terms of multiplicative white noise. Ahmaadov and Mahmud [22] utilized the Lipschitz condition to establish a sequential proof of the existence of neutral fractional SDEs.

Generally, SDEs are difficult to be solved analytically and numerical solutions are employed to afford approximate solutions of good accuracy. In this regard, researchers have constructed effective numerical techniques to obtain highly precise numerical results of different types of these equations; for example, Khodabin et al. [23] used the Taylor scheme to approximate the exact solutions of appointed type of stochastic Volterra integral equations, Kamrani [24] employed the Galerkin–Jacobi method to solve fractional SDEs numerically, Kouhkani et al. [25] developed the operational Tau method to provide numerical solutions for fractional SIDEs, Mohammadi [26] utilized the Chebyshev wavelets to solve a certain class of SIDEs, Cardone et al. [27] constructed the spectral method for solving fractional SDEs, Mirzaee and Hoseini [28] introduced the operational Fibonacci matrices to deal with nonlinear SIDEs, and Asgari et al. [29] proposed the operational matrix algorithm and Bernstein polynomials scheme to handle nonlinear SIDEs.

In this study, we are concerned with a specific form of fractional SIDEs of the Volterra type where the derivative is taken to be in the CFD sense. We prove that the existence of a stochastic process satisfies the given equation using the idea of Picard iterations with the use of some topological theorems based on reasonable conditions, and we ensure its uniqueness. Also, a numerical solution based on the SLPs as the basis of the well-known spectral collocation technique is constructed. Indeed, the convergence of the presented algorithm is proved. Anyhow, we study the fractional SIDE of the following form:

$$\begin{cases} T_{\varkappa}\mathbb{U}(\mathbb{T},\omega) = \mathfrak{F}_1(\mathbb{T},\mathbb{U}(\mathbb{T},\omega),\omega) + \lambda\int_0^{\mathbb{T}} \mathfrak{F}_2(\eta,\mathbb{U}(\eta,\omega),\omega)\mathrm{d}B_\eta, \\ \mathbb{U}(0,\omega) = \mathbb{U}_0. \end{cases} \tag{1}$$

Herein, $T \in \mathrm{I} =: [0,\mathscr{T}]$, $\omega \in \Omega$, λ is a real constant, $B = \{B(\mathbb{T})\colon \mathbb{T} \geq 0\}$ is the SBM built on a given space $(\Omega, \mathscr{F}, P)$ wherein the increasing filtration $\{\mathscr{F}_{\mathbb{T}}\}_{0\leq\mathbb{T}\leq\mathscr{T}}$ is right continuous. Indeed, Ω is the set of all possible outcomes, and P is a measure defined on $\mathscr{F}$ and satisfies $P(\mathscr{F}_{\mathscr{T}}) = 1$. The functions $\mathfrak{F}_1$ and $\mathfrak{F}_2$ are given stochastic processes, u is to be determined, and the initial condition u_0 is a given random variable presumed to be independent of B. Ultimately, $\mathscr{T}_{\varkappa}$ denotes the CFD of order $\varkappa$ with $0 < \varkappa \leq 1$.

The spectral collocation method is considered a general approximate analytical method used to obtain numerical solutions to various types of differential equations. It is simple, accurate, and does not need a highly qualified programmer. The main principle of this method is to convert extremely difficult differential problems to systems of algebraic equations which are easy to solve. To achieve this goal, the unknown function is assumed to be a linear combination of known base functions with unknown coefficients. Then, the equation is assumed to be satisfied at reasonable collocation points in the given domain. The choice of the base functions and the collocation points affect the efficiency of the method. According to the nice properties of the Legendre polynomials and their orthogonality, they are chosen to be the basis functions of the collocation method in this work. This method was previously used in solving other forms of SDEs as in [30, 31].

The remnant sections of our research are outlined next. In Section 2, basic definitions and fundamental results of the CFD concept and stochastic processes are given. The Picard

iteration idea with the use of some known topological theorems and suitable assumptions is employed to assert the existence of a single solution of (1) in Section 3. The main aim of Section 4 is to present the SL-SCA and employ it for solving (1) numerically followed by a discussion of the convergence study. Section 5 is to provide an algorithm for the scheme presented in Section 4 and uses it to solve some illustrative examples that ensure the accuracy and applicability of the SL-SCA. Finally, in Section 6, the highlight and conclusion are dedicated.

2. Preliminaries and Principal Results

In this essential portion, we survey basic definitions, notations, and intrinsic results including CFD, stochastic Itô's calculus, and some topological spaces which are required for proving our results. Moreover, utilizing the stochastic Fubini theorem, the integral representation of (1) is implemented.

2.1. The CFD Requirements. The next mentioned definition is known to be the simplest and the most natural among all fractional derivatives definitions. Although the following definitions and results are considered for $0 < \varkappa \leq 1$, they can be generalized for any $\varkappa \in \mathbb{R}$.

Definition 1 (see [2]). The CFD of order $0 < \varkappa < 1$ for $\mathfrak{F}$: $[0, \infty[\longrightarrow \mathbb{R}$ for all $t > 0$ is

$$T_{\varkappa}(\mathfrak{F})(\mathbb{T}) = \lim_{\mathscr{E} \longrightarrow 0} \frac{\mathfrak{F}\left(\mathbb{T} + \mathscr{E}\mathbb{T}^{1-\varkappa}\right) - \mathfrak{F}(\mathbb{T})}{\mathscr{E}}. \tag{2}$$

Definition 2 (see [2]). The conformable integral operator of order $0 < \varkappa \leq 1$ of $\mathfrak{F}$: $[0, \infty[\longrightarrow \mathbb{R}$ is

$$I_0^{\varkappa}(\mathfrak{F})(\mathbb{T}) = \int_0^{\mathbb{T}} \mathfrak{F}(\eta)\eta^{\varkappa - 1}\mathrm{d}\eta. \tag{3}$$

Lemma 1 (see [2]). *Let $\mathfrak{F}, \mathfrak{G}$: $[0, \infty[\longrightarrow \mathbb{R}$ be two functions and $t > 0$. Then, for $0 < \varkappa \leq 1$ we have the following:*

(1) $T_{\varkappa}(\mathfrak{F}(\mathbb{T})) = \mathbb{T}^{1-\varkappa}\mathfrak{F}'(\mathbb{T})$ if $\mathfrak{F}$ is differentiable

(2) $I_0^{\varkappa} T_{\varkappa}\mathfrak{F}(\mathbb{T}) = \mathfrak{F}(\mathbb{T}) - \mathfrak{F}(0)$ if $T_{\varkappa}\mathfrak{F}(t)$ is continuous

(3) $T_{\varkappa} I_0^{\varkappa}\mathfrak{F}(\mathbb{T}) = \mathfrak{F}(\mathbb{T})$ if $\mathfrak{F}$ is continuous

(4) $T_{\varkappa}(a\mathfrak{F} + b\mathfrak{G}) = aT_{\varkappa}(\mathfrak{F}) + bT_{\varkappa}(\mathfrak{G})$ if $\mathfrak{F}, \mathfrak{G}$ are $\varkappa$-differentiable with $a, b \in \mathbb{R}$

Herein, $\mathfrak{F}$ is called $\varkappa$-differentiable at a fixed point t when $T_{\varkappa}(\mathfrak{F})(\mathbb{T})$ exists. Indeed, a function could be $\varkappa$-differentiable for some value of $\varkappa$ at a point but not differentiable. For example, in $\mathfrak{F}(\mathbb{T}) = 2\sqrt{\mathbb{T}}$, $T_{0.5}(\mathfrak{F})(0) = 1$, but $T_1(\mathfrak{F})(0)$ does not exist.

2.2. Itô's Calculus. Stochastic calculus is a new subfield of mathematics that is concerned with stochastic processes. The most useful and applicable stochastic process is the SBM. Itô's integral which requires Itô's lemma is of big importance and lies in its ability to apply the dominated convergence theorem that is needed for proving the results of equations concerning random terms. Following that, we present the main concepts of stochastic calculus needed in the sequel.

Definition 3 (see [30]). A real-valued stochastic process $B(\mathbb{T})$ with $\mathbb{T} \in \mathrm{I}$ defines an SBM if the following subsequence properties are satisfied:

(1) For all $\mathbb{T} \in \mathrm{I}$, the increment $B(\mathbb{T} + \mathbb{H}) - B(\mathbb{T}) \sim N(0, \mathbb{H})$, where $N(\mu, \sigma^2)$ denotes the normal distribution with mean μ and variance σ^2 wherein $\mathbb{H} > 0$

(2) Distinct increments constructed of $B(\mathbb{T})$ are independent for $0 \leq \mathbb{T}_0 \leq \mathbb{T}_1 \leq \cdots \leq \mathbb{T}_{\mathbb{N}} \leq \mathscr{T}$

(3) $B(\mathbb{T})$ is almost surely a continuous function of t

(4) $B(0) = 0$ WP1

Definition 4 (see [29]). Let $\mathscr{V}(S, \mathscr{T})$ symbolize the space of all functions $\mathfrak{F}(\eta, \omega)$: $[0, \infty[\times \Omega \longrightarrow \mathbb{R}$. Then, we can utilize Itô's integral of $\mathfrak{F}$ as

$$\int_0^{\mathscr{T}} \mathfrak{F}\psi_{\mathbb{N}}(\eta, \omega)\mathrm{d}B_{\eta} = \lim_{\mathbb{N} \longrightarrow \infty} \int_0^{\mathscr{T}} \psi_{\mathbb{N}}(\eta, \omega)\mathrm{d}B_{\eta}, \tag{4}$$

where $\{\psi_{\mathbb{N}}\}_{\mathbb{N}=1}^{\infty}$ is the sequence of elementary functions, which satisfies

$$E\int_0^{\mathbb{T}} \left(\mathfrak{F} - \psi_{\mathbb{N}}\right)^2 \mathrm{d}\eta \longrightarrow 0 \text{ as } \mathbb{N} \longrightarrow \infty. \tag{5}$$

Lemma 2 (see [29]). *For $\mathfrak{F}(\eta, \omega) \in \mathscr{V}(S, \mathscr{T})$, Itô's Isometry is given by*

$$E\left(\int_0^{\mathbb{T}} \mathfrak{F}(\eta, \omega)\mathrm{d}B_{\eta}\right)^2 = E\int_0^{\mathbb{T}} \mathfrak{F}^2(\eta, \omega)\mathrm{d}\eta, \quad \mathbb{T} \in I. \tag{6}$$

2.3. Spaces and Notations. Let E denote the expected value of a random variable and $\mathfrak{G}(\mathbb{T}, \omega)$: $(\Omega, \mathscr{F}, P) \longrightarrow \mathbb{R}$ be a random function; then, the norm of $\mathfrak{G}(\mathbb{T}, \omega)$ is defined as $\mathfrak{G}(\mathbb{T}, \omega)_E = (E|\mathfrak{G}(\mathbb{T}, \omega)|^2)^{0.5}$. Let $L^2(\Omega, \mathbb{R})$ refers to the space of each random function $\mathfrak{G}(\mathbb{T}, \omega)$ wherein $E\int_0^{\mathscr{T}} |\mathfrak{G}(\mathbb{T}, \omega)|^2 \mathrm{d}\mathbb{T} < \infty$. Hereafter, the space of each $\mathscr{F}_t$-measurable, bounded, and continuous functions realized on I to $L^2(\Omega, \mathbb{R})$ is denoted by $\mathbb{C}_b = \mathbb{C}(I, L^2(\Omega, \mathbb{R}))$.

Clearly, the metric space $(\mathbb{C}_b, d)$ with $d = \max_{\mathbb{T} \in I} \mathbb{U}(\mathbb{T}) - \mathbb{W}(\mathbb{T})$ and $\mathbb{U}, \mathbb{W} \in \mathbb{C}_b$ is separable and complete. Also, the notation $(M^2(\Omega, \mathbb{C}_b), D)$ refers to the space of $\mathbb{C}_b$-valued random variables equipped with a metric D. Finally, the functions $\mathfrak{F}_1(\mathbb{T}, \mathbb{U}, \omega), \mathfrak{F}_2(\mathbb{T}, \mathbb{U}, \omega)$: $I \times \mathbb{C}_b \times \Omega \longrightarrow \mathbb{R}$ are assumed to be $L^2(\Omega, \mathbb{R})$ jointly measurable and continuous for all $\mathbb{T} \in I, \mathbb{U} \in \mathbb{C}_b$ and almost everywhere $\omega \in \Omega$, and $\|\mathbb{U}_0\|E < \infty$. This information can be found in [20].

2.4. Integral Representation and Basic Lemmas. This section is to establish an integral form of (1) and state Gronwall's inequality which is used in completing the desired proofs.

Lemma 3. *If $\mathbb{T}(\mathbb{U})$ is a solution of (1), then its integral form is*

$$\mathbb{U}(\mathbb{T},\omega)=\mathbb{U}_0+\int_0^{\mathbb{T}}\eta^{\varkappa-1}\mathfrak{F}_1(\eta,\mathbb{U}(\eta,\omega),\omega)\mathrm{d}\eta+\frac{\lambda}{\varkappa}\int_0^{\mathbb{T}}(\mathbb{T}^{\varkappa}-\eta^{\varkappa})\mathfrak{F}_2(\eta,\mathbb{U}(\eta,\omega),\omega)\mathrm{d}B_{\eta}. \tag{7}$$

Proof. Applying (3) for both sides of (1) and using the stochastic Fubini theorem [32], one gained

$$\begin{aligned}\mathbb{U}(\mathbb{T},\omega)&=\mathbb{U}_0+\int_0^{\mathbb{T}}\eta^{\varkappa-1}\mathfrak{F}_1(\eta,\mathbb{U}(\eta,\omega),\omega)\mathrm{d}\eta+\lambda\int_0^{\mathbb{T}}\int_0^{\tau}\mathfrak{F}_2(\eta,\mathbb{U}(\eta,\omega),\omega)\mathrm{d}B_{\eta}\tau^{\varkappa-1}\mathrm{d}\tau\\&=\mathbb{U}_0+\int_0^{\mathbb{T}}\eta^{\varkappa-1}\mathfrak{F}_1(\eta,\mathbb{U}(\eta,\omega),\omega)\mathrm{d}\eta+\lambda\int_0^{\mathbb{T}}\int_{\tau}^{\mathbb{T}}\eta^{\varkappa-1}d\eta\mathfrak{F}_2(\tau,\mathbb{U}(\tau,\omega),\omega)\mathrm{d}B_{\tau}\\&=\mathbb{U}_0+\int_0^{\mathbb{T}}\eta^{\varkappa-1}\mathfrak{F}_1(\eta,\mathbb{U}(\eta,\omega),\omega)\mathrm{d}\eta+\frac{\lambda}{\varkappa}\int_0^{\mathbb{T}}(\mathbb{T}^{\varkappa}-\eta^{\varkappa})\mathfrak{F}_2(\eta,\mathbb{U}(\eta,\omega),\omega)\mathrm{d}B_{\eta}.\end{aligned} \tag{8}$$

□

Lemma 4 (see [33]). *Let $\beta(\mathbb{T})$ and $\mu(\mathbb{T})$ be two non-negative continuous functions on* I *and assume that $a\geq 0$. If $\mu(\mathbb{T})\leq a+\int_0^{\mathbb{T}}\beta(\eta)\mu(\eta)d\eta$ with $t\in$ I, then Gronwall's inequality is*

$$\mu(\mathbb{T})\leq ae^{\int_0^{\mathbb{T}}\beta(\eta)\mathrm{d}\eta}. \tag{9}$$

3. Existence and Uniqueness Results

The main target of this section is to establish reasonable proof of under-growth and Lipschitz assumptions asserting the existence of a single solution of (1). Our proofs are performed using the Picard iteration scheme which goes back to Emile Picard 1856–1941. Some topological theorems and lemmas are also used. Herein, $\varkappa$ is presumed to be >0.5.

Theorem 1. *Suppose that the growth condition $E|\mathfrak{F}_i(\eta,\mathbb{U}(\eta,\omega),\omega)|^2\leq N_i(1+E|\mathbb{U}(\eta,\omega)|^2)$ with $N_i>0$ and $i=1,2$ holds; then, (1) has a solution in $\mathfrak{C}_b$.*

Proof. Using the integral form (7) and defining the Picard sequence $\{\mathbb{U}_n\}_{n=0}^{\infty}$ on I with $\mathbb{U}_0(\mathbb{T},\omega)=\mathbb{U}_0$ as

$$\mathbb{U}_{\mathbb{N}}(\mathbb{T},\omega)=\mathbb{U}_0+\int_0^{\mathbb{T}}\eta^{\varkappa-1}\mathfrak{F}_1\left(\eta,\mathbb{U}_{\mathbb{N}-1}(\eta,\omega),\omega\right)\mathrm{d}\eta+\frac{\lambda}{\varkappa}\int_0^{\mathbb{T}}(\mathbb{T}^{\varkappa}-\eta^{\varkappa})\mathfrak{F}_2\left(\eta,\mathbb{U}_{\mathbb{N}-1}(\eta,\omega),\omega\right)\mathrm{d}B_{\eta},\quad \mathbb{N}=1,2,\ldots, \tag{10}$$

and let $\max_{i=1,2}N_i\leq N^*$ for some $N^*>0$.

Step 1: we show that $\{\mathbb{U}_{\mathbb{N}}\}_{\mathbb{N}=0}^{\infty}$ is well-defined and measurable for $\mathbb{T}\in$ I. First, we denote

$$\begin{cases}\mathscr{I}_1=\displaystyle\int_0^{\mathbb{T}}\eta^{\varkappa-1}\mathfrak{F}_1\left(\eta,\mathbb{U}_{\mathbb{N}-1}(\eta,\omega),\omega\right)\mathrm{d}\eta,\\[2ex]\mathscr{I}_2=\dfrac{\lambda}{\varkappa}\displaystyle\int_0^{\mathbb{T}}(\mathbb{T}^{\varkappa}-\eta^{\varkappa})\mathfrak{F}_2\left(\eta,\mathbb{U}_{\mathbb{N}-1}(\eta,\omega),\omega\right)\mathrm{d}B_{\eta}.\end{cases} \tag{11}$$

Since $\mathfrak{F}_1$ and $\mathfrak{F}_2$ are assumed to be in $L_2(\Omega,\mathbb{R})$, and the kernels $\eta^{\varkappa-1}$ and $(\mathbb{T}^{\varkappa}-\eta^{\varkappa})$ are bounded. Then, the growth condition asserts that

$$\begin{cases}\displaystyle\int_0^{\mathbb{T}}E\left|\eta^{\varkappa-1}\mathfrak{F}_1\left(\eta,\mathbb{U}_{\mathbb{N}-1}(\eta,\omega),\omega\right)\right|^2\mathrm{d}\eta<\infty,\\[2ex]\displaystyle\int_o^{\mathbb{T}}E\left|(\mathbb{T}^{\varkappa}-\eta^{\varkappa})\mathfrak{F}_2\left(\eta,\mathbb{U}_{\mathbb{N}-1}(\eta,\omega),\omega\right)\right|^2\mathrm{d}\eta<\infty,\end{cases} \tag{12}$$

which indicates that Lebesgue's integral $\mathscr{I}_1$ and Itô's integral $\mathscr{I}_2$ are well-defined. Consequently, the sequence $\{\mathbb{U}_{\mathbb{N}}\}_{\mathbb{N}=0}^{\infty}$ is well-defined.

It remains to prove the measurability of the considered sequence. This can be explained by the measurability of $\mathfrak{F}_1$ and $\mathfrak{F}_2$, and the product of measurable continuous functions is again measurable. So, the maps

$$\begin{cases} \omega \longrightarrow \mathscr{I}_1, \\ \omega \longrightarrow \mathscr{I}_2, \end{cases} \tag{13}$$

are measurable. Thus, we deduce the requirement.

Step 2: we show that $\{\mathbb{U}_{\mathbb{N}}\}_{\mathbb{N}=0}^{\infty}$ is bounded. With the use of CSI, Itô's isometry, and the growth constraint, (10) gives

$$\begin{aligned} E\left|\mathbb{U}_{\mathbb{N}}(\mathbb{T})\right|^2 &= E\left|\mathbb{U}_0 + \int_0^{\mathbb{T}} \eta^{\varkappa-1}\mathfrak{F}_1\left(\eta, \mathbb{U}_{\mathbb{N}-1}(\eta,\omega),\omega\right)\mathrm{d}\eta + \frac{\lambda}{\varkappa}\int_0^{\mathbb{T}} \left(\mathbb{T}^{\varkappa}-\eta^{\varkappa}\right)\mathfrak{F}_2\left(\eta, \mathbb{U}_{\mathbb{N}-1}(\eta,\omega),\omega\right)\mathrm{d}B_{\eta}\right|^2 \\ &\le 3E\left|\mathbb{U}_0\right|^2 + 3\mathrm{E}\left|\int_0^{\mathbb{T}} \eta^{\varkappa-1}\mathfrak{F}_1\left(\eta, \mathbb{U}_{n-1}(\eta,\omega),\omega\right)\mathrm{d}\eta\right|^2 + 3E\left|\frac{\lambda}{\varkappa}\int_0^{\mathbb{T}} \left(\mathbb{T}^{\varkappa}-\eta^{\varkappa}\right)\mathfrak{F}_2\left(\eta, \mathbb{U}_{\mathbb{N}-1}(\eta,\omega),\omega\right)\mathrm{d}B_{\eta}\right|^2 \\ &\le 3E\left|\mathbb{U}_0\right|^2 + 3\mathscr{T}\int_0^{\mathbb{T}} \eta^{2\varkappa-2}E\left|\mathfrak{F}_1\left(\eta, \mathbb{U}_{\mathbb{N}-1}(\eta,\omega),\omega\right)\right|^2\mathrm{d}\eta + \frac{3\lambda^2}{\varkappa^2}\int_0^{\mathbb{T}} \left(\mathbb{T}^{\varkappa}-\eta^{\varkappa}\right)^2 E\left|\mathfrak{F}_2\left(\eta, \mathbb{U}_{\mathbb{N}-1}(\eta,\omega),\omega\right)\right|^2\mathrm{d}\eta \\ &\le 3E\left|\mathbb{U}_0\right|^2 + 3\mathscr{T}N^*\int_0^{\mathbb{T}} \eta^{2\varkappa-2}\left(E\left|\mathbb{U}_{\mathbb{N}-1}(\eta,\omega)\right|^2+1\right)\mathrm{d}\eta + \frac{3N^*\lambda^2}{\varkappa^2}\int_0^{\mathbb{T}} \left(\mathbb{T}^{\varkappa}-\eta^{\varkappa}\right)^2\left(E\left|\mathbb{U}_{\mathbb{N}-1}(\eta,\omega)\right|^2+1\right)\mathrm{d}\eta \\ &\le 3E\left|\mathbb{U}_0\right|^2 + 3N^*\mathscr{T}\frac{\mathscr{T}^{2\varkappa-1}}{2\varkappa-1} + 3N^*\mathscr{T}\int_0^{\mathbb{T}} \eta^{2\varkappa-2}E\left|\mathbb{U}_{\mathbb{N}-1}(\eta,\omega)\right|^2\mathrm{d}\eta + \frac{3N^*\lambda^2}{\varkappa^2}\frac{\mathscr{T}^{2\varkappa+1}}{2\varkappa+1} \\ &\quad + \frac{3N^*\lambda^2}{\varkappa^2}\int_0^{\mathbb{T}} \left(\mathbb{T}^{\varkappa}-\eta^{\varkappa}\right)^2 E\left|\mathbb{U}_{\mathbb{N}-1}(\eta,\omega)\right|^2\mathrm{d}\eta \\ &= 3E\left|u_0\right|^2 + 3N^*\mathscr{T}\frac{\mathscr{T}^{2\varkappa-1}}{2\varkappa-1} + \frac{3N^*\lambda^2}{\varkappa^2}\frac{\mathscr{T}^{2\varkappa+1}}{2\varkappa+1} + 3N^*\int_0^t\left(\mathscr{T}\eta^{2\varkappa-2} + \left(\lambda\frac{t^{\varkappa}-\eta^{\varkappa}}{\varkappa}\right)^2\right)E\left|u_{n-1}(\eta,\omega)\right|^2\mathrm{d}\eta \\ &= \mathbb{H}_1 + \mathbb{H}_2\int_0^{\mathbb{T}}\left(\mathscr{T}\eta^{2\varkappa-2} + \left(\lambda\frac{\mathbb{T}^{\varkappa}-\eta^{\varkappa}}{\varkappa}\right)^2\right)E\left|\mathbb{U}_{\mathbb{N}-1}(\eta,\omega)\right|^2\mathrm{d}\eta, \end{aligned} \tag{14}$$

where $\mathbb{H}_1 = 3E|\mathbb{U}_0|^2 + 3N^*\mathscr{T}(\mathscr{T}^{2\varkappa-1}/2\varkappa-1) + ((3N^*\lambda^2/\varkappa^2)(\mathscr{T}^{2\varkappa+1}/2\varkappa+1))$ and $\mathbb{H}_2 = 3N^*$. Also, for arbitrary $p \ge 1$, obviously,

$$\max_{1\le\mathbb{N}\le\mathbb{P}} E\left|\mathbb{U}_{\mathbb{N}-1}(\mathbb{T},\omega)\right|^2 \le \max_{1\le\mathbb{N}\le\mathbb{P}} E\left|\mathbb{U}_{\mathbb{N}}(\mathbb{T},\omega)\right|^2. \tag{15}$$

Therefore, taking the maximum of both sides of (14) one has

$$\max_{1\le\mathbb{N}\le\mathbb{P}} E\left|\mathbb{U}_{\mathbb{N}}(\mathbb{T},\omega)\right|^2 \le \mathbb{H}_1 + \mathbb{H}_2\int_0^{\mathbb{T}}\left(\mathscr{T}\eta^{2\varkappa-2} + \left(\lambda\frac{\mathbb{T}^{\varkappa}-\eta^{\varkappa}}{\varkappa}\right)^2\right)\max_{1\le\mathbb{N}\le\mathbb{P}} E\left|\mathbb{U}_{\mathbb{N}}(\mathbb{T},\omega)\right|^2\mathrm{d}\eta. \tag{16}$$

By Gronwall's inequality, we have

$$\max_{1\le\mathbb{N}\le\mathbb{P}} E\left|\mathbb{U}_{\mathbb{N}}(\mathbb{T},\omega)\right|^2 \le \mathbb{H}_1 e^{\mathbb{H}_2\int_0^{\mathbb{T}}\left(\mathscr{T}\eta^{2\varkappa-2} + \left(\lambda\mathbb{T}^{\varkappa}-\eta^{\varkappa}/\varkappa\right)^2\right)\mathrm{d}\eta} \le \mathbb{H}_1 e^{\mathbb{H}_2\mathscr{T}^{2\varkappa}\left((1/(2\varkappa-1))+\mathscr{T}\lambda^2/(2\varkappa+1)\varkappa^2\right)} < \infty. \tag{17}$$

Since $\wp$ was arbitrary, we have $E|\mathbb{U}_{\mathbb{N}}(\mathbb{T},\omega)|^2 < \infty$ which guarantees the boundedness of $\{\mathbb{U}_{\mathbb{N}}\}_{\mathbb{N}=0}^{\infty}$. Moreover, $\{\mathbb{U}_{\mathbb{N}}\}_{\mathbb{N}=0}^{\infty}$ is uniformly bounded.

Step 3: we prove the equicontinuity of $\{\mathbb{U}_{\mathbb{N}}\}_{\mathbb{N}=0}^{\infty}$. Let $0 < \mathbb{T}_1 < \mathbb{T}_2 < \mathscr{T}$, $\mathbb{T}_2 - \mathbb{T}_1 < \delta_*$, and $\max_{0<\mathbb{T}<\mathscr{T}} 1 + E|\mathbb{U}_{\mathbb{N}-1}(\mathbb{T},\omega)|^2 \le \vartheta, \vartheta > 1$. Let $\epsilon > 0$ be given and choose $\delta > 0$ such that $0 < (\delta_*)^{2\varkappa}\ ((1/2\varkappa - 1) + (2\lambda^2\delta_*/\varkappa^2(2\varkappa+1)) + (2\mathscr{T}\lambda^2/\varkappa^2)) \le \delta$ and

$$\delta \le \frac{\epsilon}{2\vartheta N^*}. \tag{18}$$

Employing CSI, Itô's isometry, and (10), one obtains

$$\begin{aligned}
\left|\mathbb{U}_{\mathbb{N}}(\mathbb{T}_2,\omega) - \mathbb{U}_{\mathbb{N}}(\mathbb{T}_1,\omega)\right|^2 &\le 2\left|\int_0^{\mathbb{T}_2} \eta^{\varkappa-1}\mathfrak{F}_1(\eta,\mathbb{U}_{\mathbb{N}-1}(\eta,\omega)\omega)\mathrm{d}\eta - \int_0^{\mathbb{T}_1} \eta^{\varkappa-1}\mathfrak{F}_1(\eta,\mathbb{U}_{\mathbb{N}-1}(\eta,\omega),\omega)\mathrm{d}\eta\right|^2 \\
&\quad + \frac{2\lambda^2}{\varkappa^2}\left|\int_0^{\mathbb{T}_2}((\mathbb{T}_2)^{\varkappa} - \eta^{\varkappa})\mathfrak{F}_2(\eta,\mathbb{U}_{\mathbb{N}-1}(\eta,\omega),\omega)\mathrm{d}B_\eta - \int_0^{\mathbb{T}_1}((\mathbb{T}_1)^{\varkappa} - \eta^{\varkappa})\mathfrak{F}_2(\eta,\mathbb{U}_{\mathbb{N}-1}(\eta,\omega),\omega)\mathrm{d}B_\eta\right|^2 \\
&\le 2\left|\int_{\mathbb{T}_1}^{\mathbb{T}_2} \eta^{\varkappa-1}\mathfrak{F}_1(\eta,\mathbb{U}_{\mathbb{N}-1}(\eta,\omega),\omega)\mathrm{d}\eta\right|^2 \\
&\quad + \frac{4\lambda^2}{\varkappa^2}\left|\int_{\mathbb{T}_1}^{\mathbb{T}_2}((\mathbb{T}_2)^{\varkappa} - \eta^{\varkappa})\mathfrak{F}_2(\eta,\mathbb{U}_{\mathbb{N}-1}(\eta,\omega),\omega)\mathrm{d}B_\eta\right|^2 \\
&\quad + \frac{4\lambda^2}{\varkappa^2}\left|\int_0^{\mathbb{T}_1}((\mathbb{T}_2)^{\varkappa} - (\mathbb{T}_1)^{\varkappa})\mathfrak{F}_2(\eta,\mathbb{U}_{\mathbb{N}-1}(\eta,\omega),\omega)\mathrm{d}B_\eta\right|^2.
\end{aligned} \tag{19}$$

Taking the expectation of both sides, one has

$$\begin{aligned}
&E\left|u_n(t_2,\omega) - u_n(t_1,\omega)\right|^2 \\
E\left|\mathbb{U}_{\mathbb{N}}(\mathbb{T}_2,\omega) - \mathbb{U}_{\mathbb{N}}(\mathbb{T}_1,\omega)\right|^2 &\le 2\int_{\mathbb{T}_1}^{\mathbb{T}_2}\eta^{2\varkappa-2}\mathrm{d}\eta\int_{\mathbb{T}_1}^{\mathbb{T}_2}E\left|\mathfrak{F}_1(\eta,\mathbb{U}_{n-1}(\eta,\omega),\omega)\right|^2\mathrm{d}\eta \\
&\quad + \frac{4\lambda^2}{\varkappa^2}\int_{\mathbb{T}_1}^{\mathbb{T}_2}((\mathbb{T}_2)^{\varkappa} - \eta^{\varkappa})^2 E\left|\mathfrak{F}_2(\eta,\mathbb{U}_{\mathbb{N}-1}(\eta,\omega),\omega)\right|^2 d\eta \\
&\quad + \frac{4\lambda^2}{\varkappa^2}(\mathbb{T}_2 - \mathbb{T}_1)^{2\varkappa}\int_0^{\mathbb{T}_1}E\left|\mathfrak{F}_2(\eta,\mathbb{U}_{\mathbb{N}-1}(\eta,\omega),\omega)\right|^2\mathrm{d}\eta \\
&\le \frac{2}{2\varkappa-1}\left((\mathbb{T}_2)^{2\varkappa-1} - (\mathbb{T}_1)^{2\varkappa-1}\right)\int_{\mathbb{T}_1}^{\mathbb{T}_2}E\left|\mathfrak{F}_1(\eta,\mathbb{U}_{\mathbb{N}-1}(\eta,\omega),\omega)\right|^2\mathrm{d}\eta \\
&\quad + \frac{4\lambda^2}{\varkappa^2}\int_{\mathbb{T}_1}^{\mathbb{T}_2}((\mathbb{T}_2)^{\varkappa} - \eta^{\varkappa})^2 E\left|\mathfrak{F}_2(\eta,\mathbb{U}_{\mathbb{N}-1}(\eta,\omega),\omega)\right|^2\mathrm{d}\eta \\
&\quad + \frac{4\lambda^2}{\varkappa^2}(\mathbb{T}_2 - \mathbb{T}_1)^{2\varkappa}\int_0^{\mathbb{T}_1}E\left|\mathfrak{F}_2(\eta,\mathbb{U}_{\mathbb{N}-1}(\eta,\omega),\omega)\right|^2\mathrm{d}\eta
\end{aligned}$$

$$
\begin{aligned}
&\leq \frac{2}{2\varkappa-1}\left(\mathbb{T}_2-\mathbb{T}_1\right)^{2\varkappa-1}N^*\int_{\mathbb{T}_1}^{\mathbb{T}_2}\left(1+E\left|\mathbb{U}_{\mathbb{N}-1}(\eta,\omega)\right|^2\right)\mathrm{d}\eta\\
&\quad+\frac{4N^*\lambda^2}{\varkappa^2}\int_{\mathbb{T}_1}^{\mathbb{T}_2}\left(\mathbb{T}_2-\eta\right)^{2\varkappa}\left(1+E\left|\mathbb{U}_{\mathbb{N}-1}(\eta,\omega)\right|^2\right)\mathrm{d}\eta\\
&\quad+\frac{4N^*\lambda^2}{\varkappa^2}\left(\mathbb{T}_2-\mathbb{T}_1\right)^{2\varkappa}\int_0^{\mathbb{T}_1}\left(1+E\left|\mathbb{U}_{\mathbb{N}-1}(\eta,\omega)\right|^2\right)\mathrm{d}\eta\\
&\leq \frac{2N^*\vartheta}{2\varkappa-1}\left(\mathbb{T}_2-\mathbb{T}_1\right)^{2\varkappa}\\
&\quad+\frac{4\lambda^2N^*\vartheta}{\varkappa^2(2\varkappa+1)}\left(\mathbb{T}_2-\mathbb{T}_1\right)^{2\varkappa+1}\\
&\quad+\frac{4\mathcal{T}\lambda^2N^*\vartheta}{\varkappa^2}\left(\mathbb{T}_2-\mathbb{T}_1\right)^{2\varkappa}\\
&\leq 2N^*\vartheta\left(\delta_*\right)^{2\varkappa}\left(\frac{1}{2\varkappa-1}+\frac{2\lambda^2\delta_*}{\varkappa^2(2\varkappa+1)}+\frac{2\mathcal{T}\lambda^2}{\varkappa^2}\right)\\
&\leq 2N^*\vartheta\delta.
\end{aligned}
\tag{20}
$$

By (18), one gets $E|\mathbb{U}_{\mathbb{N}}(\mathbb{T}_2,\omega)-\mathbb{U}_{\mathbb{N}}(\mathbb{T}_1,\omega)|^2\leq\epsilon$ which proves the equicontinuity of $\{\mathbb{U}_{\mathbb{N}}\}_{\mathbb{N}=0}^{\infty}$.

Step 4: by the results gained in Steps 2 and 3, Arzela-Ascoli's theorem assures that $\{\mathbb{U}_{\mathbb{N}}\}_{\mathbb{N}=0}^{\infty}$ is a compact subset of $\mathcal{C}_b$. In addition, Step 2 asserts the boundedness of the sequence $\{\mathbb{U}_{\mathbb{N}}\}_{\mathbb{N}=0}^{\infty}$ which indicates that $\mathbb{U}_{\mathbb{N}}\in M_2(\Omega,\mathcal{C}_b)$. Applying Prohorov's theorem, one gets the totally D-boundedness of the sequence $\{\mathbb{U}_{\mathbb{N}}\}_{\mathbb{N}=0}^{\infty}$ in $M_2(\Omega,\mathcal{C}_b)$. Thus, $\{\mathbb{U}_{\mathbb{N}}\}_{\mathbb{N}=0}^{\infty}$ has a D-Cauchy subsequence $\{\mathbb{U}_{\mathbb{N}_{\mathbb{M}}}\}_{\mathbb{N}=0}^{\infty}$ denoted by $\{\mathbb{U}_{\mathbb{M}}\}_{\mathbb{M}=1}^{\infty}$ [34]. Then, Skorokhod's representation lemma [35] assures the existence of a convergence sequence $\{\mathbb{W}_{\mathbb{M}}\}_{\mathbb{M}=1}^{\infty}$ in $M_2(\Omega,\mathcal{C}_b)$ that has the same distribution as $\{\mathbb{U}_{\mathbb{M}}\}_{\mathbb{M}=1}^{\infty}$ such that the following subsequence properties are satisfied:

(1) $D(\mathbb{W}_{\mathbb{M}},\mathbb{U}_{\mathbb{M}})=0$, $\mathbb{M}=1,2,\ldots$

(2) $\mathbb{W}_{\mathbb{M}}\longrightarrow\mathbb{U}$ WP1 as $\mathbb{M}\longrightarrow\infty$ for some continuous $\mathcal{F}_{\partial}$-measurable random variable $\mathbb{U}$ in $M_2(\Omega,\mathcal{C}_b)$

The abovementioned properties ensure the boundedness of $\mathbb{W}_{\mathbb{M}}$ and $\mathbb{U}$ WP1. Now, it remains to prove that $\mathbb{U}$, the limit of $\{\mathbb{W}_{\mathbb{M}}\}_{\mathbb{M}=1}^{\infty}$, satisfies (1). For this end, we consider the following:

$$
\begin{aligned}
E\left|\mathbb{W}_{\mathbb{M}}(\mathbb{T},\omega)-\mathbb{U}(\mathbb{T},\omega)\right|^2&=E\left|\int_0^{\mathbb{T}}\eta^{\varkappa-1}\left(\mathfrak{F}_1(\eta,\mathbb{W}_{\mathbb{M}}(\eta,\omega),\omega)-\mathfrak{F}_1(\eta,\mathbb{U}(\eta,\omega),\omega)\right)\mathrm{d}\eta+\frac{\lambda}{\varkappa}\int_0^{\mathbb{T}}\left(\mathbb{T}^{\varkappa}-\eta^{\varkappa}\right)\left(\mathfrak{F}_2(\eta,\mathbb{W}_{\mathbb{M}}(\eta,\omega),\omega)-\mathfrak{F}_2(\eta,\mathbb{U}(\eta,\omega),\omega)\right)\mathrm{d}B_{\eta}\right|^2\\
&\leq 2E\left|\int_0^{\mathbb{T}}\eta^{\varkappa-1}\left(\mathfrak{F}_1(\eta,\mathbb{W}_{\mathbb{M}}(\eta,\omega),\omega)-\mathfrak{F}_1(\eta,\mathbb{U}(\eta,\omega),\omega)\right)\mathrm{d}\eta\right|^2\\
&\quad+\frac{2\lambda^2}{\varkappa^2}E\left|\int_0^{\mathbb{T}}\left(\mathbb{T}^{\varkappa}-\eta^{\varkappa}\right)\left(\mathfrak{F}_2(\eta,\mathbb{W}_{\mathbb{M}}(\eta,\omega),\omega)-\mathfrak{F}_2(\eta,\mathbb{U}(\eta,\omega),\omega)\right)\mathrm{d}B_{\eta}\right|^2\\
&\leq 2\int_0^{\mathbb{T}}\eta^{2\varkappa-2}\mathrm{d}\eta\int_0^{\mathbb{T}}E\left|\mathfrak{F}_1(\eta,\mathbb{W}_{\mathbb{M}}(\eta,\omega),\omega)-\mathfrak{F}_1(\eta,\mathbb{U}(\eta,\omega),\omega)\right|^2\mathrm{d}\eta
\end{aligned}
$$

$$+\frac{2\lambda^2}{\varkappa^2}\int_0^{\mathbb{T}}\left(\mathbb{T}^{\varkappa}-\eta^{\varkappa}\right)^2 E\left|\mathfrak{F}_2\left(\eta,\mathbb{W}_{\mathbb{M}}(\eta,\omega),\omega\right)-\mathfrak{F}_2\left(\eta,\mathbb{U}(\eta,\omega),\omega\right)\right|^2 \mathrm{d}\eta$$

$$\leq\frac{2\mathscr{T}^{2\varkappa-1}}{2\varkappa-1}\int_0^{\mathscr{T}} E\left|\mathfrak{F}_1\left(\eta,\mathbb{W}_{\mathbb{M}}(\eta,\omega),\omega\right)-\mathfrak{F}_1\left(\eta,\mathbb{U}(\eta,\omega),\omega\right)\right|^2 \mathrm{d}\eta$$

$$+\frac{2\lambda^2}{\varkappa^2}\int_0^{\mathscr{T}}\left(\mathscr{T}^{\varkappa}-\eta^{\varkappa}\right)^2 E\left|\mathfrak{F}_2\left(\eta,\mathbb{W}_{\mathbb{M}}(\eta,\omega),\omega\right)-\mathfrak{F}_2\left(\eta,\mathbb{U}(\eta,\omega),\omega\right)\right|^2 \mathrm{d}\eta. \tag{21}$$

By the continuity of $\mathfrak{F}_1$ and $\mathfrak{F}_2$, it appears that for given $\varepsilon>0$, $\exists i\geq 0$ with i integer such that, for $\mathbb{M}>i$,

$$\begin{aligned}\int_0^{\mathscr{T}} E\left|\mathfrak{F}_1\left(\eta,\mathbb{W}_{\mathbb{M}}(\eta,\omega),\omega\right)-\mathfrak{F}_1\left(\eta,\mathbb{U}(\eta,\omega),\omega\right)\right|^2 \mathrm{d}\eta &\leq \mathscr{T}\frac{\epsilon}{2},\\ \int_0^{\mathscr{T}}\left(\mathscr{T}^{\varkappa}-\eta^{\varkappa}\right)^2 E\left|\mathfrak{F}_2\left(\eta,\mathbb{W}_{\mathbb{M}}(\eta,\omega),\omega\right)-\mathfrak{F}_2\left(\eta,\mathbb{U}(\eta,\omega),\omega\right)\right|^2 \mathrm{d}\eta &\leq \frac{\mathscr{T}^{2\varkappa+1}}{2\varkappa+1}\frac{\epsilon}{2}.\end{aligned} \tag{22}$$

Hence, for all $\mathbb{T}\in \mathrm{I}$, one has

$$\int_0^{\mathbb{T}}\eta^{\varkappa-1}\mathfrak{F}_1\left(\eta,\mathbb{W}_{\mathbb{M}}(\eta,\omega),\omega\right)\mathrm{d}\eta = \longrightarrow \int_0^{\mathbb{T}}\eta^{\varkappa-1}\mathfrak{F}_1\left(\eta,\mathbb{U}(\eta,\omega),\omega\right)\mathrm{d}\eta, \tag{23}$$

$$\int_0^{\mathbb{T}}\left(\mathbb{T}^{\varkappa}-\eta^{\varkappa}\right)\mathfrak{F}_2\left(\eta,\mathbb{W}_{\mathbb{M}}(\eta,\omega),\omega\right)\mathrm{d}B_{\eta} \longrightarrow \int_0^{\mathbb{T}}\left(\mathbb{T}^{\varkappa}-\eta^{\varkappa}\right)\mathfrak{F}_2\left(\eta,\mathbb{U}(\eta,\omega),\omega\right)\mathrm{d}B_{\eta}. \tag{24}$$

With the property $D(\mathbb{W}_{\mathbb{M}},\mathbb{U}_{\mathbb{M}})=0$ within $\mathbb{M}=1,2,\ldots$ mentioned in Step 4, (10) yields

$$\mathbb{W}_{\mathbb{M}}(\mathbb{T},\omega)=\mathbb{U}_0+\int_0^{\mathbb{T}}\eta^{\varkappa-1}\mathfrak{F}_1\left(\eta,\mathbb{W}_{\mathbb{M}-1}(\eta,\omega),\omega\right)\mathrm{d}\eta+\frac{\lambda}{\varkappa}\int_0^{\mathbb{T}}\left(\mathbb{T}^{\varkappa}-\eta^{\varkappa}\right)\mathfrak{F}_2\left(\eta,\mathbb{W}_{\mathbb{M}-1}(\eta,\omega),\omega\right)\mathrm{d}B_{\eta}. \tag{25}$$

Letting $\mathbb{M}\longrightarrow\infty$, relations (23)–(25), and the property $\mathbb{W}_{\mathbb{M}}\longrightarrow\mathbb{U}$ WP1 shows that

$$\begin{aligned}\mathbb{U}(\mathbb{T},\omega)=\mathbb{U}_0&+\int_0^{\mathbb{T}}\eta^{\varkappa-1}\mathfrak{F}_1\left(\eta,\mathbb{U}(\eta,\omega),\omega\right)\mathrm{d}\eta\\ &+\frac{\lambda}{\varkappa}\int_0^{\mathbb{T}}\left(\mathbb{T}^{\varkappa}-\eta^{\varkappa}\right)\mathfrak{F}_2\left(\eta,\mathbb{U}(\eta,\omega),\omega\right)\mathrm{d}B_{\eta}.\end{aligned} \tag{26}$$

Consequently, (26) demonstrates that $\mathbb{U}(\mathbb{T},\omega)$ is a random solution of (1) as required. □

Theorem 2. *Under the Lipschitz assumption* $E|\mathfrak{F}_2(\eta,\mathbb{W}(\eta,\omega),\omega) - \mathfrak{F}_2(\eta,\mathbb{U}(\eta,\omega),\omega)|^2 \leq LE|\mathbb{W}(\eta,\omega) - \mathbb{U}(\eta,\omega)|^2$ *with* $L>0$ *the solution of (1) is unique.*

Proof. Let $\mathbb{W}(\mathbb{T},\omega)$ and $\mathbb{U}(\mathbb{T},\omega)$ be two solutions to (1). Then, using the integral form (7), one has

$$
\begin{aligned}
E|\mathbb{W}(\mathbb{T},\omega)-\mathbb{U}(\mathbb{T},\omega)|^2 &= E\left|\int_0^{\mathbb{T}} \eta^{\varkappa-1}\left(\mathfrak{F}_1(\eta,\mathbb{W}(\eta,\omega),\omega)-\mathfrak{F}_1(\eta,\mathbb{U}(\eta,\omega),\omega)\right)\mathrm{d}\eta+\frac{\lambda}{\varkappa}\int_0^{\mathbb{T}}\left(\mathbb{T}^{\varkappa}-\eta^{\varkappa}\right)\left(\mathfrak{F}_2(\eta,\mathbb{W}(\eta,\omega),\omega)-\mathfrak{F}_2(\eta,\mathbb{U}(\eta,\omega),\omega)\right)\mathrm{d}B_{\eta}\right|^2\\
&\le 2E\left|\int_0^{\mathbb{T}} \eta^{\varkappa-1}\left(\mathfrak{F}_1(\eta,\mathbb{W}(\eta,\omega),\omega)-\mathfrak{F}_1(\eta,\mathbb{U}(\eta,\omega),\omega)\right)\mathrm{d}\eta\right|^2\\
&\quad+\frac{2\lambda^2}{\varkappa^2}E\left|\int_0^{\mathbb{T}}\left(\mathbb{T}^{\varkappa}-\eta^{\varkappa}\right)\left(\mathfrak{F}_2(\eta,\mathbb{W}(\eta,\omega),\omega)-\mathfrak{F}_2(\eta,\mathbb{U}(\eta,\omega),\omega)\right)\mathrm{d}B_{\eta}\right|^2\\
&\le 2\int_0^{\mathbb{T}}\eta^{2\varkappa-2}\mathrm{d}\eta\int_0^{\mathbb{T}}E\left|\mathfrak{F}_1(\eta,\mathbb{W}(\eta,\omega),\omega)-\mathfrak{F}_1(\eta,\mathbb{U}(\eta,\omega),\omega)\right|^2\mathrm{d}\eta\\
&\quad+\frac{2\lambda^2}{\varkappa^2}\int_0^{\mathbb{T}}\left(\mathbb{T}^{\varkappa}-\eta^{\varkappa}\right)^2E\left|\mathfrak{F}_2(\eta,\mathbb{W}(\eta,\omega),\omega)-\mathfrak{F}_2(\eta,\mathbb{U}(\eta,\omega),\omega)\right|^2\mathrm{d}\eta\\
&\le\frac{2\mathscr{T}^{2\varkappa-1}}{2\varkappa-1}\int_0^{\mathbb{T}}E\left|\mathfrak{F}_1(\eta,\mathbb{W}(\eta,\omega),\omega)-\mathfrak{F}_1(\eta,\mathbb{U}(\eta,\omega),\omega)\right|^2\mathrm{d}\eta\\
&\quad+\frac{2\lambda^2}{\varkappa^2}\int_0^{\mathbb{T}}\left(\mathbb{T}^{\varkappa}-\eta^{\varkappa}\right)^2E\left|\mathfrak{F}_2(\eta,\mathbb{W}(\eta,\omega),\omega)-\mathfrak{F}_2(\eta,\mathbb{U}(\eta,\omega),\omega)\right|^2\mathrm{d}\eta.
\end{aligned}
\tag{27}
$$

Again, by the Lipschitz condition, one has

$$
\begin{aligned}
E|\mathbb{W}(\mathbb{T},\omega)-\mathbb{U}(\mathbb{T},\omega)|^2 &\le\frac{2\mathscr{T}^{2\varkappa-1}}{2\varkappa-1}L\int_0^{\mathbb{T}}E|\mathbb{W}(\eta,\omega)-\mathbb{U}(\eta,\omega)|^2\mathrm{d}\eta\\
&\quad+\frac{2\lambda^2}{\varkappa^2}L\int_0^{\mathbb{T}}\left(\mathbb{T}^{\varkappa}-\eta^{\varkappa}\right)^2E|\mathbb{W}(\eta,\omega)-\mathbb{U}(\eta,\omega)|^2\mathrm{d}\eta\\
&=2L\int_0^{\mathbb{T}}\left(\frac{\mathscr{T}^{2\varkappa-1}}{2\varkappa-1}+\left(\lambda\frac{\mathbb{T}^{\varkappa}-\eta^{\varkappa}}{\varkappa}\right)^2\right)E|\mathbb{W}(\eta,\omega)-\mathbb{U}(\eta,\omega)|^2\mathrm{d}\eta.
\end{aligned}
\tag{28}
$$

Applying Gronwall's inequality on (28), one yields

$$
E|\mathbb{W}(\mathbb{T},\omega)-\mathbb{U}(\mathbb{T},\omega)|^2\le 0. \tag{29}
$$

Hence, $\mathbb{W}(\mathbb{T},\omega)=\mathbb{U}(\mathbb{T},\omega)$ for all $\mathbb{T}\in \mathrm{I}$. So, the uniqueness has been proved. □

4. Numerical Solution and Convergence Analysis

Unlike the deterministic FDEs, which have deterministic solutions, fractional SIDEs solutions are continuously stochastic processes. Aside from differences, solving fractional SIDEs numerically is based on similar techniques that are used for deterministic ones. Herein, the SL-SCA is discussed in detail and employed to grant the numerical solutions of (1). It is indispensable to focus on the fact that each trajectory provided by the presented method is just one realization of the exact stochastic process satisfying (1). To confirm the convergence of the presented algorithm when solving (1), we construct a theorem and apply Gronwall's inequality in proving it.

4.1. Adaptive SL-SCA for Fractional SIDEs. The spectral collocation technique is considered one of the most applicable numerical methods that provide high-precision numerical solutions for various types of FDEs. The main idea of its algorithm is to derive a system of a finite number of algebraic equations by assuming the unknown function to be a truncated series of some suitable basis functions with unknown coefficients. Because of the simplicity, smoothness, and orthogonality properties of the Legendre polynomials, they are selected to be the base functions of the algorithm discussed in the current section.

To fulfill the goal of approximating the unknown function $\mathbb{U}(\mathbb{T},\omega)$ in (1), we first present a review of the SLPs and state a theorem that asserts the ability to approximate unknown functions by SLPs expansions. In this sense, the unknown function $\mathbb{U}(\mathbb{T},\omega)$ in (1) is replaced by a finite series of SLPs resulting in a residual error function $\mathrm{Res}(\mathbb{T})$ which is assumed to be zero at a suitable choice of collocation points. In addition, the finite series satisfies the initial conditions. Accordingly, (1) is converted to a facilely solvable system of algebraic equations. For simplicity of notation, the variable ω is dropped and we write $\mathbb{U}(\mathbb{T})$, $\mathfrak{F}_1(\mathbb{T},\mathbb{U}(\mathbb{T}))$, and

$\mathfrak{F}_2(\mathbb{T}, \mathbb{U}(\mathbb{T}))$ instead of $\mathbb{U}(\mathbb{T}, \omega)$, $\mathfrak{F}_1(\mathbb{T}, \mathbb{U}(\mathbb{T}, \omega), \omega)$, and $\mathfrak{F}_2(\mathbb{T}, \mathbb{U}(\mathbb{T}, \omega), \omega)$, respectively.

Legendre polynomials are known to be built on $[-1, 1]$. Utilizing appropriate change of variables, Legendre polynomials can be restricted to $[0, 1]$ and then called the SLPs. They satisfy the orthogonality property concerning the weight function $w(\mathbb{T}) = 1$. SLPs can be expressed in a recursive formula [36] but the most efficient formula is the following analytical series [37]:

$$\mathbb{K}_{\mathbb{P}}(\mathbb{T}) = \sum_{\mathbb{Q}=0}^{\mathbb{P}} (-1)^{\mathbb{P}+\mathbb{Q}} \frac{1}{(\mathbb{P}-\mathbb{Q})!(\mathbb{Q}!)^2} (\mathbb{P}+\mathbb{Q})! \mathbb{T}^{\mathbb{Q}}, \quad \mathbb{P} = 0, 1, \ldots. \tag{30}$$

The orthogonality property of SLPs over $[0, 1]$ is

$$\int_0^1 \mathbb{K}_i(\mathbb{T}) \mathbb{K}_{\mathbb{P}}(\mathbb{T}) \mathrm{d}\mathbb{T} = \begin{cases} (2i+1)^{-1}, & i = \mathbb{P}, \\ 0, & i \neq \mathbb{P}. \end{cases} \tag{31}$$

Definition 5 (see [38]). For all $\mathbb{U}, \mathbb{W} \in L_2[0, 1]$ the functional of $L_2[0, 1]$ is

$$\begin{cases} \mathbb{U}|\mathbb{W} = \int_0^1 \mathbb{U}(\mathbb{T}) \mathbb{W}(\mathbb{T}) \mathrm{d}\mathbb{T}, \\ \mathbb{U}_{L_2} = \sqrt{\mathbb{U}|\mathbb{U}}. \end{cases} \tag{32}$$

Theorem 3 (see [36]). *Let $P_N = \{P_i, i \leq N\}$, where P_i is a polynomial of degree i. Then, for $\mathbb{W} \in L_2[0, 1]$, there is a unique polynomial $q_N^* \in P_N$ such that*

$$\mathbb{W} - q_{NL_2}^* = \inf_{q_N \in P_N} \mathbb{W} - q_{NL_2}, \tag{33}$$

where $q_N^*(\mathbb{T}) = \sum_{i=0}^{N} \gamma_i \varphi_i(\mathbb{T})$ with $\gamma_i = (\mathbb{W}|\varphi_i / \|\varphi_i\|_{L_2})$ and the sequence $\{\varphi_i\}_{i=1}^{N}$ is an orthogonal basis for P_N in the L_2 space.

Since they satisfy the orthogonality property, the SLPs form an orthogonal basis for P_N in L_2 space. Thus, the previous theorem asserts that $\mathbb{U}(\mathbb{T}) \in L_2[0, 1]$ can be uniquely approximated by a truncated series of the SLPs as follows:

$$\begin{aligned} \mathbb{U}(\mathbb{T}) &\cong \mathbb{U}_N(\mathbb{T}) \\ &= \sum_{\mathbb{P}=0}^{N-1} \lambda_{\mathbb{P}} \mathbb{K}_{\mathbb{P}}(\mathbb{T}), \end{aligned} \tag{34}$$

where $\lambda_{\mathbb{P}} = (2\mathbb{P}+1)\mathbb{U}(\mathbb{T})|\mathbb{K}_{\mathbb{P}}(\mathbb{T})$ with $\mathbb{P} = 0, 1, \ldots, N-1$.

Using the linearity property of the CFD, one can easily verify that the approximation of the derivative of $\mathbb{U}_N(\mathbb{T})$ in the conformable sense is

$$\mathcal{T}_{\varkappa} \mathbb{U}_N(\mathbb{T}) = \sum_{\mathbb{P}=0}^{N-1} \lambda_{\mathbb{P}} \mathcal{T}_{\varkappa} \mathbb{K}_{\mathbb{P}}(\mathbb{T}), \tag{35}$$

$$\mathcal{T}_{\varkappa} \mathbb{K}_{\mathbb{P}}(\mathbb{T}) = \begin{cases} \sum_{\mathbb{Q}=1}^{\mathbb{P}} (-1)^{\mathbb{P}+\mathbb{Q}} \dfrac{\mathbb{Q}(\mathbb{P}+\mathbb{Q})!}{(\mathbb{P}-\mathbb{Q})!(\mathbb{Q}!)^2} \mathbb{T}^{\mathbb{Q}-\varkappa}, & \mathbb{P} = 1, 2, \ldots, \\ 0, & \mathbb{P} = 0. \end{cases} \tag{36}$$

Also, using the property $\int_0^1 \mathbb{H}(\eta) \mathrm{d}B_S = \mathbb{H}(\mathbb{T}) B(\mathbb{T}) - \int_0^{\mathbb{T}} B(\eta) \mathrm{d}\mathbb{H}_\eta$ Itô's integral in (1) can be written as

$$\int_0^{\mathbb{T}} \mathfrak{F}_2(\eta, \mathbb{U}(\eta)) \mathrm{d}B_S = \mathfrak{F}_2(\mathbb{T}, \mathbb{U}(\mathbb{T})) B(\mathbb{T}) - \int_0^{\mathbb{T}} \frac{\partial \mathfrak{F}_2(\eta, \mathbb{U}(\eta))}{\partial \eta} B(\eta) \mathrm{d}\eta. \tag{37}$$

Inserting relations (34), (35), and (37) into (1), it leads to

$$\mathrm{Res}_N(\mathbb{T}) = \sum_{\mathbb{P}=0}^{N-1} \lambda_{\mathbb{T}} ABCD_0^{\alpha} \mathbb{K}_{\mathbb{P}}(\mathbb{T}) - \mathfrak{F}\left(\mathbb{T}, \sum_{\mathbb{P}=0}^{N-1} \lambda_{\mathbb{P}} \mathbb{K}_{\mathbb{P}}(\mathbb{T})\right) - \mathfrak{G}\left(\mathbb{T}, \sum_{\mathbb{P}=0}^{N-1} \lambda_{\mathbb{P}} \mathbb{K}_{\mathbb{P}}(\mathbb{T})\right) B(\mathbb{T}) + \int_0^{\mathbb{T}} \frac{\partial \mathfrak{F}_2\left(\eta, \sum_{\mathbb{P}=0}^{N-1} \lambda_{\mathbb{P}} \mathbb{K}_{\mathbb{P}}(\eta)\right)}{\partial \eta} B(\eta) \mathrm{d}\eta, \tag{38}$$

where $\mathrm{Res}_N(\mathbb{T})$ denotes the residual error function that is produced when substituting $\mathbb{U}_N(\mathbb{T})$ in (1).

Now, for $i = 1, 2, \ldots, N-1$, we substitute each collocation point $\mathbb{T}_i$, arranged as $\mathbb{T}_i < \mathbb{T}_{i+1}$, into (38) and get

$$\mathrm{Res}_N(\mathbb{T}_i) = \sum_{\mathbb{P}=0}^{N-1} \lambda_{\mathbb{P}} D_0^{\alpha} \mathbb{K}_{\mathbb{P}}(\mathbb{T}_i) - \mathfrak{F}_1\left(\mathbb{T}_i, \sum_{\mathbb{P}=0}^{N-1} \lambda_{\mathbb{P}} \mathbb{K}_{\mathbb{P}}(\mathbb{T}_i)\right) - \mathfrak{F}_2\left(\mathbb{T}_i, \sum_{\mathbb{P}=0}^{N-1} \lambda_{\mathbb{P}} \mathbb{K}_{\mathbb{P}}(\mathbb{T}_i)\right) B(\mathbb{T}_i) + \int_0^{\mathbb{T}_i} \frac{\partial \mathfrak{F}_2\left(\eta, \sum_{\mathbb{P}=0}^{N-1} \lambda_{\mathbb{P}} \mathbb{K}_{\mathbb{P}}(\eta)\right)}{\partial \eta} B(\eta) \mathrm{d}\eta. \tag{39}$$

To approximate the integral term in (39), one can use the composite trapezoidal rule as follows:

$$\int_0^{\mathbb{T}_i} \mathbb{H}(\eta) B(\eta) \mathrm{d}\eta \cong \frac{\mathbb{T}_i}{2i\mathbb{M}} \left[\mathbb{H}(\mathbb{T}_i) B(\mathbb{T}_i) + 2 \sum_{\mathbb{P}=1}^{i\mathbb{M}-1} \mathbb{H}\left(\mathbb{P}\frac{\mathbb{T}}{i\mathbb{M}}\right) B\left(\mathbb{P}\frac{\mathbb{T}_{\mathbb{P}}}{i\mathbb{M}}\right)\right], \tag{40}$$

where $\mathbb{M} \geq 2$ is an integer and $\mathbb{H}(\eta) = \partial \mathfrak{F}_2(\eta, \mathbb{U}_N(\eta))/\partial \eta$.

Anyhow, the substituting of (40) into (39), leads to

$$\begin{aligned} \mathrm{Res}_N(\mathbb{T}_i) + \varepsilon_{\mathbb{M}}(\mathbb{T}_i) = {} & \sum_{\mathbb{P}=0}^{N-1} \lambda_{\mathbb{P}} \mathscr{T}_{\varkappa} \mathbb{K}_{\mathbb{P}}(\mathbb{T}) - \mathfrak{F}_1\left(\mathbb{T}_i, \sum_{\mathbb{P}=0}^{N-1} \lambda_{\mathbb{P}} \mathbb{K}_{\mathbb{P}}(\mathbb{T}_i)\right) - \mathfrak{F}_2\left(\mathbb{T}_i, \sum_{\mathbb{P}=0}^{N-1} \lambda_{\mathbb{P}} \mathbb{K}_{\mathbb{P}}(\mathbb{T}_i)\right) B(\mathbb{T}_i) \\ & + \frac{\mathbb{T}_i}{2i\mathbb{M}} \left[\mathbb{H}(\mathbb{T}_i) B(\mathbb{T}_i) + 2 \sum_{\mathbb{P}=1}^{i\mathbb{M}-1} \mathbb{H}\left(\mathbb{P}\frac{\mathbb{T}_{\mathbb{P}}}{i\mathbb{M}}\right) B\left(\mathbb{P}\frac{\mathbb{T}_{\mathbb{P}}}{i\mathbb{M}}\right)\right], \end{aligned} \tag{41}$$

where $\varepsilon_{\mathbb{M}}(\mathbb{T}_i)$ is the trapezoidal rule error related to the integral approximating using (39). It is known that $\varepsilon_{\mathbb{M}}(\mathbb{T}_i) \longrightarrow 0$ as $\mathbb{M} \longrightarrow \infty$.

Now, for $i = 1, 2, \ldots, N-1$ one has

$$\begin{aligned} 0 = {} & \sum_{\mathbb{P}=0}^{N-1} \lambda_{\mathbb{P}} \mathscr{T}_{\varkappa} \mathbb{K}_{\mathbb{P}}(\mathbb{T}_i) - \mathfrak{F}_1\left(\mathbb{T}_i, \sum_{\mathbb{P}=0}^{N-1} \lambda_{\mathbb{P}} \mathbb{K}_{\mathbb{P}}(\mathbb{T}_i)\right) - \mathfrak{F}_2\left(\mathbb{T}_i, \sum_{\mathbb{P}=0}^{N-1} \lambda_{\mathbb{P}} \mathbb{K}_{\mathbb{P}}(\mathbb{T}_i)\right) B(\mathbb{T}_i) \\ & + \frac{\mathbb{T}_i}{2i\mathbb{M}} \left[\mathbb{H}(\mathbb{T}_i) B(\mathbb{T}_i) + 2 \sum_{\mathbb{P}=1}^{i\mathbb{M}-1} \mathbb{H}\left(\mathbb{P}\frac{\mathbb{T}_{\mathbb{P}}}{i\mathbb{M}}\right) B\left(\mathbb{P}\frac{\mathbb{T}_{\mathbb{P}}}{i\mathbb{M}}\right)\right]. \end{aligned} \tag{42}$$

The property $\mathbb{K}_{\mathbb{P}}(0) = (-1)^{\mathbb{P}}$ together with the initial condition gives

$$\sum_{\mathbb{P}=0}^{N-1} \lambda_{\mathbb{P}} (-1)^{\mathbb{P}} = \mathbb{U}_0. \tag{43}$$

Hence, (42) and (43) form a system containing N algebraic equations. This system has solved the unknowns $\lambda_{\mathbb{P}}$ wherein $\mathbb{P} = 0, 1, \ldots, N-1$ with the aid of a suitable

method. Consequently, the approximate solution of (1), when substituting the values of $\lambda_{\mathbb{P}}$ in (34), is obtained.

It remains to treat a crucial issue of simulating the SBM sample paths over an appropriate discretization $0 < \mathbb{T}_1 < \ldots < \mathbb{T}_{\mathbb{P}} < \ldots < \mathbb{T}_{\tau}$ of I, for a positive integer τ. The discretization is considered to be equally spaced with $\mathbb{T}_{\mathbb{P}} - \mathbb{T}_{\mathbb{P}-1} = (\mathscr{T}/\tau) = \Delta\mathbb{T}$ wherein $\mathbb{P} = 1, \ldots, \tau$ and then $B(\mathbb{T}_{\mathbb{P}}) - B(\mathbb{T}_{\mathbb{P}-1}) = dB(\mathbb{T}_{\mathbb{P}}) \sim \mathrm{N}(0, \Delta\mathbb{T})$. To obtain an approximate value for $B(\mathbb{T})$, a linear spline interpolation [30] is then applied using the points $(\mathbb{T}_{\mathbb{P}}, B(\mathbb{T}_{\mathbb{P}}))$ wherein $\mathbb{P} = 0, 1, \ldots, \tau$.

4.2. Convergence of SL-SCA. This part is to emphasize the convergence of the proposed algorithm. For this aim, it is initially proven that the finite Legendre series expansion of a function in $L^2[0,1]$ converges and has finite modulus coefficients. Then, proof of convergence of SL-SCA considering (1) is constructed.

Theorem 4. *The Legendre expansion* $\sum_{\mathbb{P}=0}^{N} \lambda_{\mathbb{P}} \mathbb{K}_{\mathbb{P}}(\mathbb{T})$ *of* $\mathbb{U}(\mathbb{T}) \in L^2[0,1]$ *converges to* $\mathbb{U}(\mathbb{T})$ *as* $N \longrightarrow \infty$.

Proof. Let $\mathbb{U}_{\mathfrak{M}}(\mathbb{T}) = \sum_{\mathbb{P}=0}^{\mathfrak{M}} \lambda_{\mathbb{P}} \mathbb{K}_{\mathbb{P}}(\mathbb{T})$. Then, for $N > \mathfrak{M}$, we have

$$\begin{aligned}
\left\| \mathbb{U}_N(x) - \mathbb{U}_{\mathfrak{M}}(x) \right\|_{L_2}^2 &= \left\| \sum_{\mathbb{P}=\mathfrak{M}+1}^{N} \lambda_{\mathbb{P}} \mathbb{K}_{\mathbb{P}}(\mathbb{T}) \right\|_{L_2}^2 \\
&= \left\langle \sum_{\mathbb{P}=\mathfrak{M}+1}^{N} \lambda_{\mathbb{P}} \mathbb{K}_{\mathbb{P}}(\mathbb{T}) \middle| \sum_{i=\mathfrak{M}+1}^{N} \lambda_i \mathbb{K}_i(\mathbb{T}) \right\rangle \\
&= \sum_{\mathbb{P}=\mathfrak{M}+1}^{N} \sum_{i=\mathfrak{M}+1}^{N} \lambda_{\mathbb{P}} \overline{\lambda_i} \langle \mathbb{K}_{\mathbb{P}}(\mathbb{T}) | \mathbb{K}_i(\mathbb{T}) \rangle \\
&= \sum_{\mathbb{P}=\mathfrak{M}+1}^{N} \sum_{\mathbb{P}=\mathfrak{M}+1}^{N} \lambda_{\mathbb{P}} \overline{\lambda_i} \int_0^1 \mathbb{K}_{\mathbb{P}}(\mathbb{T}) \mathbb{K}_i(\mathbb{T}) \mathrm{d}\mathbb{T} \\
&= \sum_{\mathbb{P}=\mathfrak{M}+1}^{N} |\lambda_{\mathbb{P}}|^2 \left(\frac{1}{2\mathbb{P}+1} \right) < \sum_{\mathbb{P}=\mathfrak{M}+1}^{N} |\lambda_{\mathbb{P}}|^2.
\end{aligned} \tag{44}$$

Bessel's inequality indicates that $\sum_{\mathbb{P}=\mathfrak{M}+1}^{N} |\lambda_{\mathbb{P}}|^2 \leq \sum_{\mathbb{P}=\mathfrak{M}+1}^{\infty} |\lambda_{\mathbb{P}}|^2 \leq \mathbb{U}_{L_2}^2 < \infty$. So, $\mathbb{U}_N(\mathbb{T}) - \mathbb{U}_{\mathfrak{M}}(\mathbb{T})_{L_2}^2 \longrightarrow 0$ as $N, \mathfrak{M} \longrightarrow \infty$. Thus, the sequence $\mathbb{U}_N(\mathbb{T})$ is Cauchy in the complete space $L^2[0,1]$ and converges to some $\mathbb{W}(\mathbb{T}) \in L^2[0,1]$. Now, to show $\mathbb{W}(\mathbb{T}) = \mathbb{U}(\mathbb{T})$, we consider

$$\begin{aligned}
\langle \mathbb{W}(\mathbb{T}) - \mathbb{U}(\mathbb{T}) | \mathbb{K}_{\mathbb{P}}(\mathbb{T}) \rangle &= \langle \mathbb{W}(\mathbb{T}) | \mathbb{K}_{\mathbb{P}}(\mathbb{T}) \rangle - \langle \mathbb{W}(\mathbb{T}) | \mathbb{K}_{\mathbb{P}}(\mathbb{T}) \rangle \\
&= \lim_{N \longrightarrow \infty} \langle \mathbb{U}_N(\mathbb{T}), \mathbb{K}_{\mathbb{P}}(\mathbb{T}) \rangle - \lambda_{\mathbb{P}} \\
&= \lambda_{\mathbb{P}} - \lambda_{\mathbb{P}}, \\
&= 0.
\end{aligned} \tag{45}$$

Hence, $\mathbb{W}(\mathbb{T}) = \mathbb{W}(\mathbb{T})$ which completes the proof. □

Theorem 5. *Weconsider* $\mathbb{U}(\mathbb{T}, \omega)$ *and* $\mathbb{U}_N(\mathbb{T}, \omega)$ *concerning (1) and suppose that the Lipschitz condition* $E|\mathfrak{F}_2(\eta, \mathbb{U}(\eta, \omega), \omega) - \mathfrak{F}_2(\eta, \mathbb{U}_N(\eta, \omega), \omega)|^2 \leq LE|\mathbb{U}(\eta, \omega) - \mathbb{U}_N(\eta, \omega)|^2$, $L > 0$, *is satisfied. Then,*

$$\mathbb{U}(\mathbb{T}, \omega) - \mathbb{U}_N(\mathbb{T}, \omega)_2 \longrightarrow 0 \text{ as } N \longrightarrow \infty. \tag{46}$$

Proof. Let $e_N(\mathbb{T}, \omega) = \mathbb{U}(\mathbb{T}, \omega) - \mathbb{U}_N(\mathbb{T}, \omega)$ be the error function results when the exact solution $\mathbb{U}(\mathbb{T}, \omega)$ of (1) is approximated by $\mathbb{U}_N(\mathbb{T})$ that is given in (34). So, using (7), we have

$$\begin{aligned} e_N(\mathbb{T},\omega) &= \mathbb{U}(\mathbb{T},\omega) - \mathbb{U}_N(\mathbb{T},\omega) \\ &= \int_0^{\mathbb{T}} \eta^{\varkappa-1}\left(\mathfrak{F}_1(\eta,\mathbb{U}(\eta,\omega),\omega) - \mathfrak{F}_1\left(\eta,\mathbb{U}_N(\eta,\omega),\omega\right)\right)\mathrm{d}\eta \\ &\quad + \frac{\lambda^2}{\varkappa^2}\int_0^{\mathbb{T}}\left(\mathbb{T}^{\varkappa}-\eta^{\varkappa}\right)\left(\mathfrak{F}_2(\eta,\mathbb{U}(\eta,\omega),\omega) - \mathfrak{F}_2\left(\eta,\mathbb{U}_N(\eta,\omega),\omega\right)\right)\mathrm{d}B_\eta + I_0^{\varkappa}\varepsilon_{\mathbb{M}} + I_0^{\varkappa}\mathrm{Res}_N(\mathbb{T}), \end{aligned} \tag{47}$$

The triangular inequality, CSI, and Itô's lemma give

$$\begin{aligned} &E\left|\mathbb{U}(\mathbb{T},\omega) - \mathbb{U}_N(\mathbb{T},\omega)\right|^2 \\ &= E\left|\int_0^{\mathbb{T}} \eta^{\varkappa-1}\left(\mathfrak{F}_1(\eta,\mathbb{U}(\eta,\omega),\omega) - \mathfrak{F}_1\left(\eta,\mathbb{U}_N(\eta,\omega),\omega\right)\right)\mathrm{d}\eta + \frac{\lambda}{\varkappa}\int_0^{\mathbb{T}}\left(\mathbb{T}^{\varkappa}-\eta^{\varkappa}\right)\left(\mathfrak{F}_2(\eta,\mathbb{U}(\eta,\omega),\omega) - \mathfrak{F}_2\left(\eta,\mathbb{U}_N(\eta,\omega),\omega\right)\right)\mathrm{d}B_\eta\right| \\ &\quad + I_0^{\varkappa}\varepsilon_{\mathbb{M}} + I_0^{\varkappa}\mathrm{Res}_N(\mathbb{T})^2 \\ &\le 4E\left|\int_0^{\mathbb{T}} \eta^{\varkappa-1}\left(\mathfrak{F}_1(\eta,\mathbb{U}(\eta,\omega),\omega) - \mathfrak{F}_1\left(\eta,\mathbb{U}_N(\eta,\omega),\omega\right)\right)\mathrm{d}\eta\right|^2 + \frac{4\lambda^2}{\varkappa^2}E\left|\int_0^{\mathbb{T}}\left(\mathbb{T}^{\varkappa}-\eta^{\varkappa}\right)\left(\mathfrak{F}_2(\eta,\mathbb{U}(\eta,\omega),\omega) - \mathfrak{F}_2\left(\eta,\mathbb{U}_N(\eta,\omega),\omega\right)\right)\mathrm{d}B_\eta\right|^2 \\ &\quad + 4E\left|I_0^{\varkappa}\varepsilon_{\mathbb{M}}\right|^2 + 4E\left|I_0^{\varkappa}\mathrm{Res}_N(\mathbb{T})\right|^2 \\ &\le 4\int_0^{\mathbb{T}}\eta^{2\varkappa-2}d\eta\int_0^{\mathbb{T}}E\left|\mathfrak{F}_1(\eta,\mathbb{U}(\eta,\omega),\omega) - \mathfrak{F}_1\left(\eta,\mathbb{U}_N(\eta,\omega),\omega\right)\right|^2\mathrm{d}\eta + \frac{4\lambda^2}{\varkappa^2}\int_0^{\mathbb{T}}\left(\mathbb{T}^{\varkappa}-\eta^{\varkappa}\right)^2E\left|\mathfrak{F}_2(\eta,\mathbb{U}(\eta,\omega),\omega) - \mathfrak{F}_2\left(\eta,\mathbb{U}_N(\eta,\omega),\omega\right)\right|^2d\eta \\ &\quad + 4E\left|I_0^{\varkappa}\varepsilon_{\mathbb{M}}\right|^2 + 4E\left|I_0^{\varkappa}\mathrm{Res}_N(\mathbb{T})\right|^2 \\ &\le \frac{4\mathscr{T}^{2\varkappa-1}}{2\varkappa-1}\int_0^{\mathbb{T}}E\left|\mathfrak{F}_1(\eta,\mathbb{U}(\eta,\omega),\omega) - \mathfrak{F}_1\left(\eta,\mathbb{U}_N(\eta,\omega),\omega\right)\right|^2\mathrm{d}\eta + \frac{4\lambda^2}{\varkappa^2}\int_0^{\mathbb{T}}\left(\mathbb{T}^{\varkappa}-\eta^{\varkappa}\right)^2E\left|\mathfrak{F}_2(\eta,\mathbb{U}(\eta,\omega),\omega) - \mathfrak{F}_2\left(\eta,\mathbb{U}_N(\eta,\omega),\omega\right)\right|^2\mathrm{d}\eta \\ &\quad + 4E\left|I_0^{\varkappa}\varepsilon_{\mathbb{M}}\right|^2 + 4E\left|I_0^{\varkappa}\mathrm{Res}_N(\mathbb{T})\right|^2. \end{aligned} \tag{48}$$

Now, using the Lipschitz condition and simple calculations, we otain

$$\begin{aligned} e_N(\mathbb{T})_E^2 &\le \frac{4\mathscr{T}^{2\varkappa-1}}{2\varkappa-1}L\int_0^{\mathbb{T}}E\left|\mathbb{U}(\eta,\omega) - \mathbb{U}_N(\eta,\omega)\right|^2\mathrm{d}\eta + \frac{4\lambda^2}{\varkappa^2}L\int_0^{\mathbb{T}}\left(\mathbb{T}^{\varkappa}-\eta^{\varkappa}\right)^2E\left|\mathbb{U}(\eta,\omega) - \mathbb{U}_N(\eta,\omega)\right|^2\mathrm{d}\eta + 4I_0^{\varkappa}\varepsilon_E^2 + 4I_0^{\varkappa}\mathrm{Res}_N(\mathbb{T})_E^2 \\ &= 2L\int_0^{\mathbb{T}}\left(\frac{\mathscr{T}^{2\varkappa-1}}{2\varkappa-1} + \left(\lambda\frac{\mathbb{T}^{\varkappa}-\eta^{\varkappa}}{\varkappa}\right)^2\right)e_N(\mathbb{T})_E^2\mathrm{d}\eta + 4I_0^{\varkappa}\varepsilon_E^2 + 4I_0^{\varkappa}\mathrm{Res}_N(\mathbb{T})_E^2. \end{aligned} \tag{49}$$

Let $\varrho(N,\mathbb{M}) = 4\|I_0^{\varkappa}\varepsilon_{\mathbb{M}}\|_E^2 + 4\|I_0^{\varkappa}\mathrm{Res}_N(\mathbb{T})\|_E^2$ and apply Gronwall's inequality on (49), which yields

$$e_N(\mathbb{T})_E^2 \le \varrho(N,\mathbb{M})\mathrm{e}^{\int_0^{\mathbb{T}}2L\left(\mathscr{T}^{2\varkappa-1}/2\varkappa-1+\left(\lambda\mathbb{T}^{\varkappa}-\eta^{\varkappa}/\varkappa\right)^2\right)\mathrm{d}\eta}. \tag{50}$$

Since $\varrho(N,\mathbb{M}) \longrightarrow 0$ as $N,\mathbb{M}\longrightarrow\infty$ and for $\mathbb{T}\in\mathrm{I}$, $\int_0^{\mathbb{T}}2L(\mathscr{T}^{2\varkappa-1}/2\varkappa-1+(\lambda\mathbb{T}^{\varkappa}-\eta^{\varkappa}/\varkappa)^2)\mathrm{d}\eta<\infty$. Then, $\mathbb{U}(\mathbb{T})-\mathbb{U}_N(\mathbb{T})_2\longrightarrow 0$ as $N,m\longrightarrow\infty$ as required. □

5. Numerical Results and Examples

To emphasize the results gained in previous sections, we provide an algorithm consisting of clear steps based on the SL-SCA described in Section 4 and utilize it to solve examples of linear and nonlinear forms of (1) numerically. Hither, the values of the SBM are calculated for $\tau = 128$, and for the collocation points, the subsequence formula is used [30].

$$\mathbb{T}_i = \frac{1}{2} - \frac{1}{2}\cos\left(\frac{(2i+1)\pi}{2N+2}\right), \quad i = 1, 2, \ldots, N-1. \tag{51}$$

Generally, the exact solution of (1) does not exist. So, we consider $e_N(\mathbb{T}) = |\mathbb{U}_N(\mathbb{T}) - \mathbb{U}(\mathbb{T})|$ to be the error function which is calculated only for examples that have no stochastic terms (see Example 1 for $\lambda = 0$).

Example 1. Consider the following linear fractional SIDE:

$$\begin{cases} T_{\varkappa}\mathbb{U}(\mathbb{T}) = \mathbb{U}(\mathbb{T}) + \mathbb{T}^{0.25} + 2\mathbb{T}^{1.25} - \mathbb{T}^2 - \mathbb{T} + \lambda \int_0^{\mathbb{T}} \eta \mathrm{d}B_{\eta}, \\ \mathbb{U}(0) = 0, \end{cases} \tag{52}$$

wherein $\mathbb{T} \in \mathrm{I} = [0, 1]$ and $0.5 < \varkappa < 1$. Hither, for $\varkappa = 0.75$ and $\lambda = 0$, the exact solution is $\mathbb{U}(\mathbb{T}) = \mathbb{T}^2 + \mathbb{T}$.

Example 2. Linear fractional SIDE is as follows:

$$\begin{cases} T_{\varkappa}\mathbb{U}(\mathbb{T}) = \mathbb{U}(\mathbb{T}) + \mathbb{T}^{0.5} - \mathbb{T}^2 + \int_0^{\mathbb{T}} \mathbb{U}(\eta)\mathrm{d}B_{\eta}, \\ \mathbb{U}(0) = 0, \end{cases} \tag{53}$$

wherein $\mathbb{T} \in \mathrm{I} = [0, 1]$ and $0.5 < \varkappa < 1$.

Example 3. Linear fractional SIDE is as follows:

$$\begin{cases} T_{\varkappa}\mathbb{U}(\mathbb{T}) = \mathbb{T}^2 \sin(\mathbb{T}) + \int_0^{\mathbb{T}} \mathbb{U}(\eta)\mathrm{d}B_{\eta}, \\ \mathbb{U}(0) = 0, \end{cases} \tag{54}$$

wherein $\mathbb{T} \in \mathrm{I} = [0, 1]$ and $0.5 < \varkappa < 1$.

Example 4. Nonlinear fractional SIDE is as follows:

$$\begin{cases} T_{\varkappa}\mathbb{U}(\mathbb{T}) = \mathbb{U}^2(\mathbb{T}) + \mathbb{U}(\mathbb{T}) - \mathbb{T} + \int_0^{\mathbb{T}} 0.5\mathrm{d}B_{\eta}, \\ \mathbb{U}(0) = 0, \end{cases} \tag{55}$$

wherein $t \in \mathrm{I} = [0, 1]$ and $0.5 < \varkappa < 1$.

Example 5. Nonlinear fractional SIDE is as follows:

$$\begin{cases} T_{\varkappa}t(t) = t\sqrt{t(t)} + \int_0^1 \eta \mathrm{d}B_{\eta}, \\ t(0) = 0, \end{cases} \tag{56}$$

wherein $\mathbb{T} \in \mathrm{I} = [0, 1]$ and $0.5 < \varkappa < 1$.

It is important to shed light on the fact that different SBM paths produce different approximated realizations. Fixed $\omega \in \Omega$, a path of an SBM $B(\mathbb{T}, \omega) = B(\mathbb{T})$, is a continuous nowhere differentiable starting from zero WP1 and has independent normally distributed discrete increments. As it is presented in Section 4, $B(\mathbb{T})$ can be simulated at fixed values of $\mathbb{T}$. The paths that appear in Figure 1 are performed using Mathematica 11 program.

For Example 1, the subsequence results have been obtained by employing Algorithm 1. Firstly, in Table 1, data outcomes for $\mathbb{U}_N(\mathbb{T})$ and $\mathbb{U}(\mathbb{T})$ at $N \in \{4, 6, 9\}$, $\varkappa = 0.75$, and $\lambda = 0$ are tabulated. Secondly, in Table 2, data outcomes for $\mathbb{U}_N(\mathbb{T})$ at $\varkappa \in \{0.8, 0.85, 0.9, 0.95\}$, $N = 7$, and $\lambda = 1$ are tabulated. Thirdly, in Figure 2 graphical outcomes for $\mathbb{U}_N(\mathbb{T})$, $\mathbb{U}(\mathbb{T})$, and $e_N(\mathbb{T})$ at $\lambda = 0$, $\varkappa = 0.75$, and $N = 4$ are sketched. Fourthly, in Figure 3 graphical outcomes for $\mathbb{U}_N(\mathbb{T})$, $\mathbb{U}(\mathbb{U})$, and $e_N(\mathbb{T})$ at $\lambda = 0, \varkappa = 0.75$, and $N = 9$ are sketched. Fifthly, in Figure 4 graphical outcomes for $\mathbb{U}_N(\mathbb{T})$ at $\varkappa \in \{0.80, 0.85, 0.90\}$, $N \in \{3, 4, 6\}$, and $\lambda = 1$ are sketched.

The following algorithm steps are executed using MATHEMATICA 11 software:

For Example 2, the subsequence results have been obtained by employing Algorithm 1. Firstly, in Table 3, data outcomes for $\mathbb{U}_N(\mathbb{T})$ at $\varkappa \in \{0.65, 0.7, 0.75, 0.8\}$ and $N = 3$ are tabulated. Secondly, in Figure 5, graphical outcomes for $\mathbb{U}_N(\mathbb{T})$ at $\varkappa \in \{0.65, 0.7, 0.75\}$ and $N \in \{4, 5, 6\}$ are sketched.

For Example 3, the subsequence results have been obtained by employing Algorithm 1. Firstly, in Table 4, data outcomes for $\mathbb{U}_N(\mathbb{T})$ at $\varkappa \in \{0.70, 0.75, 0.8, 0.85\}$ and $N = 5$ are tabulated. Secondly, in Figure 6, graphical outcomes for $\mathbb{U}_N(\mathbb{T})$ at $\varkappa \in (0.75, 0.80, 0.85)$ and $N \in \{4, 5, 6\}$ are sketched.

For Example 4, the subsequence results have been obtained by employing Algorithm 1. Firstly, in Table 5, data outcomes for $\mathbb{U}_N(\mathbb{T})$ at $\varkappa \in \{0.65, 0.7, 0.75, 0.8\}$ and $N = 6$

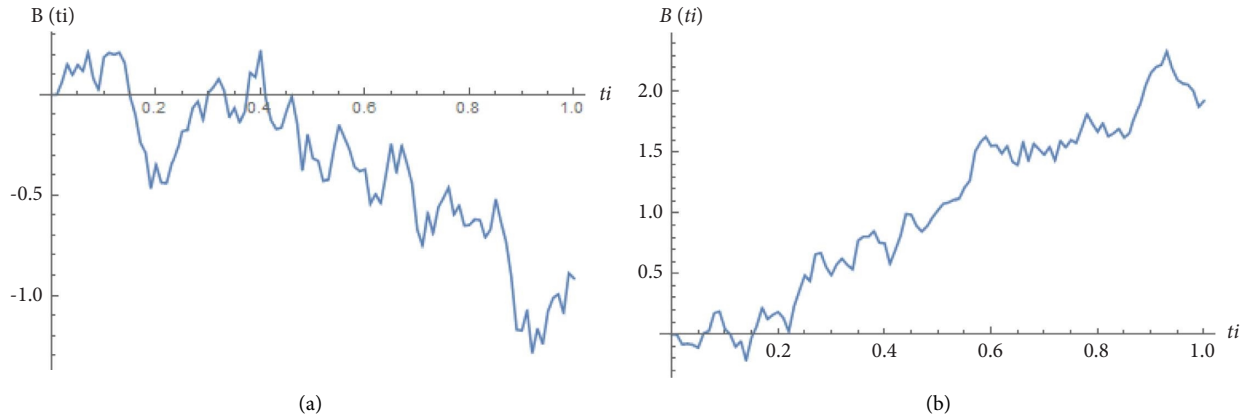

Figure 1: Path for the values of the SBM $B(\mathbb{T})$ as (a) the results shown in Examples 1–3 and (b) the results shown in Examples 4-5.

Input: Initial data: $\varkappa$, $\mathbb{M}$, $\mathcal{T}$, N, $\mathbb{U}_0, \lambda$. Functions: $\mathfrak{F}_1$, and $\mathfrak{F}_2$. SBM: B.
Execution A: Compute SLPs $\mathbb{K}_i(\mathbb{T})$ for $i = 0, 1, \cdots, N-1$ from (30).
Execution B: Compute for $T_\varkappa \mathbb{K}_i(\mathbb{T}) i = 1, 2, \cdots, N-1$ from (36).
Execution C: Compute $\mathbb{K}_i(0)$ for $i = 1, 2, \cdots, N-1$.
Execution D: Compute the collocation points $\mathbb{T}_i$ for $i = 1, 2, \cdots, N-1$ using (51).
Execution E: Approximate $\int_0^{\mathbb{T}_i} (\partial \mathfrak{F}_2(\eta, \sum_{\mathbb{P}=0}^{N-1} \lambda_{\mathbb{P}} \mathbb{K}_{\mathbb{P}}(\eta))/\partial \eta) B(\eta) \mathrm{d}\eta$ using (40).
Execution G: Solve the system of N algebraic equations of (42) and (43).
Output: The approximation $\mathbb{U}_N(\mathbb{T}) = \sum_{i=0}^{N-1} \lambda_i \mathbb{K}_i(\mathbb{T})$.

Algorithm 1: Executions of the SL-SCA in handling fractional SIDEs (1).

Table 1: Comparison results using $\mathbb{U}(\mathbb{T}_i)$ and $\mathbb{U}_N(\mathbb{T}_i)$ at $N \in \{4, 6, 9\}$, $\varkappa = 0.75$, and $\lambda = 0$ in Example 1.

t_i	$u(t_i)$	$u_4(t_i)$	$u_6(t_i)$	$u_9(t_i)$
0.1	0.11	0.1099999999999997	0.1100000000000008	0.1100000000000023
0.2	0.24	0.2399999999999998	0.24000000000000077	0.2400000000000029
0.3	0.39	0.3899999999999997	0.3900000000000009	0.3900000000000031
0.4	0.56	0.5599999999999997	0.5600000000000012	0.5600000000000036
0.5	0.75	0.7499999999999997	0.7500000000000012	0.7500000000000041
0.6	0.96	0.9599999999999996	0.9600000000000015	0.9600000000000045
0.7	1.19	1.1899999999999995	1.1900000000000015	1.1900000000000048
0.8	1.44	1.4399999999999995	1.4400000000000020	1.4400000000000055
0.9	1.71	1.7099999999999993	1.7100000000000022	1.7100000000000062
1	2	1.9999999999999991	2.0000000000000027	2.0000000000000058

Table 2: Comparison of results using $\mathbb{U}_N(\mathbb{T}_i)$ at $\varkappa \in \{0.8.85, 0.9, 0.95\}$, $N = 7$, and $\lambda = 1$ in Example 1.

$(\mathbb{T}_i, \varkappa)$	0.8	0.85	0.9	0.95
0.1	0.1825499692783584	0.1614913720931948	0.1432918550612591	0.1274765043403953
0.2	0.3120061527326218	0.2753353917003565	0.2437797812350475	0.2164647064745620
0.3	0.4533740020659298	0.4017317892835375	0.3572878935152716	0.3187941863116985
0.4	0.6242699654968027	0.5569764473353238	0.4989492254782788	0.4485718992234469
0.5	0.8181562746382847	0.7347732328068570	0.6627360559880484	0.6000590374852741
0.6	1.0219051561778874	0.9225067927018182	0.8365366726982506	0.7616378531569623
0.7	1.2276924683583443	1.1124763128363648	1.0127785723511709	0.9258684424022094
0.8	1.4392207622591702	1.3080902397650505	1.1945980978735130	1.0956354912473438
0.9	1.6722717678790247	1.5250219658726678	1.3975565122690483	1.2863849827791434
1	1.9495883050188922	1.7873264776320887	1.6469025093081697	1.5244508657817661

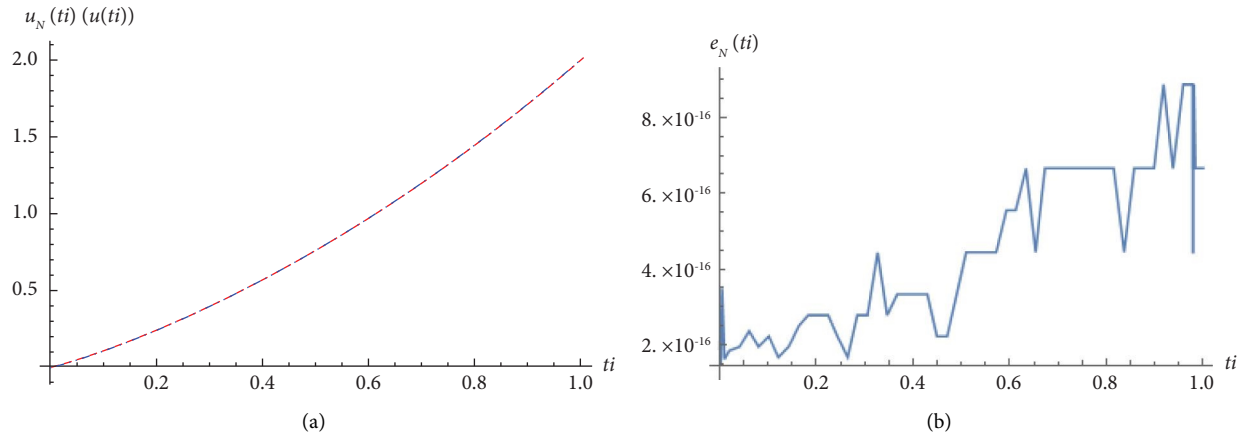

Figure 2: Schematic effects in Example 1 within $\varkappa = 0.75$, $\lambda = 0$, and $N = 4$ as (a) $\mathbb{U}_N(\mathbb{T})$ (blue) and $\mathbb{U}(\mathbb{T})$ (red) and (b) $e_N(\mathbb{T})$.

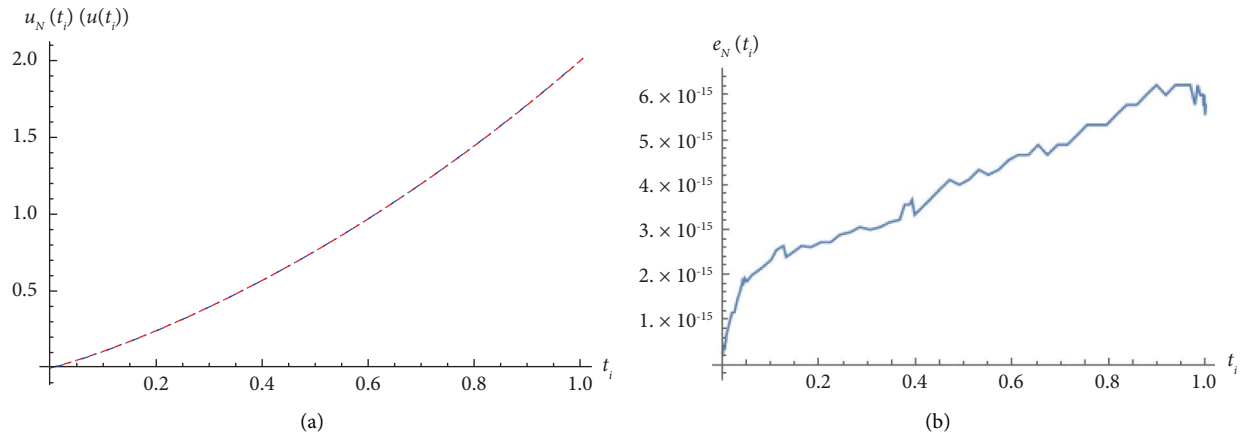

Figure 3: Schematic effects in Example 1 within $\varkappa = 0.75$, $\lambda = 0$, and $N = 9$ as (a) $\mathbb{U}_N(\mathbb{T})$ (blue) and $\mathbb{U}(\mathbb{T})$ (red) and (b) $e_N(\mathbb{T})$.

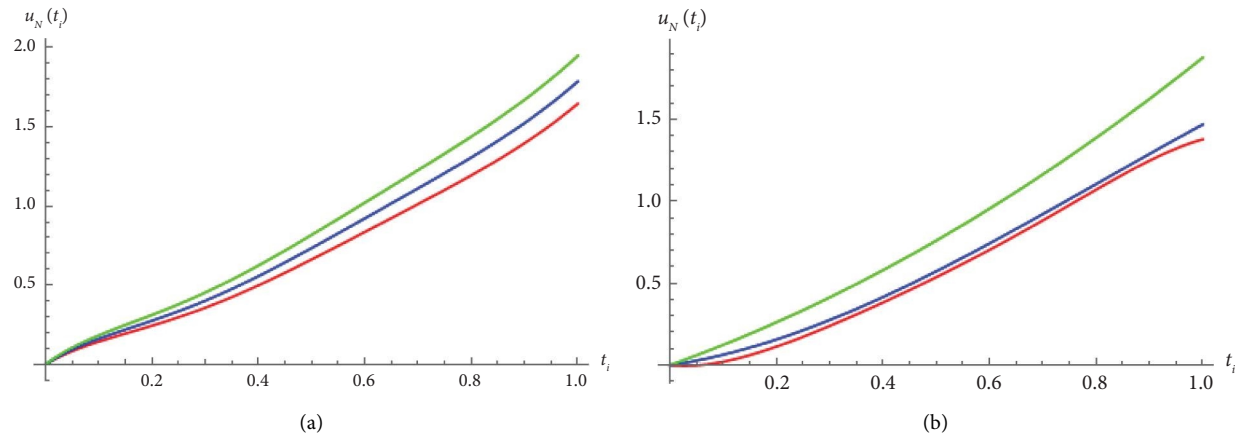

Figure 4: Schematic effects in Example 1 as (a) $\mathbb{U}_N(\mathbb{T})$ at $\varkappa \in \{0.8, 0.85, 0.9\}$, $N = 7$, and $\lambda = 1$ as red: $\varkappa = 0.9$, blue: $\varkappa = 0.85$, and green: $\varkappa = 0.8$ and (b) $\mathbb{U}_N(\mathbb{T})$ at $N \in \{3, 4, 6\}$, $\varkappa = 0.8$, and $\lambda = 1$ as red: $N = 6$, blue: $N = 4$, and green: $N = 3$.

Table 3: Comparison of results using $\mathbb{U}_N(\mathbb{T}_i)$ at $\varkappa \in \{0.65, 0.7, 0.75, 0.8\}$ and $N = 3$ in Example 2.

$(t_i, \varkappa)$	0.65	0.7	0.75	0.8
0.1	0.1479826669508654	0.1293142614636659	0.1136770713928284	0.1004124712352107
0.2	0.2935431324567124	0.2572206341298863	0.2267909897658416	0.2009732595755456
0.3	0.4366813965175409	0.3837191179986610	0.3393417551190396	0.3016823650210046
0.4	0.5773974591333513	0.5088097130699905	0.4513293674524221	0.4025397875715878
0.5	0.7156913203041431	0.6324924193438741	0.5627538267659894	0.5035455272272951
0.6	0.8515629800299166	0.7547672368203123	0.6736151330597413	0.6046995839881265
0.7	0.9850124383106715	0.8756341654993052	0.7839132863336779	0.7060019578540820
0.8	1.1160396951464087	0.9950932053808526	0.8936482865877990	0.8074526488251619
0.9	1.2446447505371268	1.1131443564649541	1.0028201338221052	0.9090516569013657
1	1.3708276044828270	1.2297876187516104	1.1114288280365956	1.0107989820826937

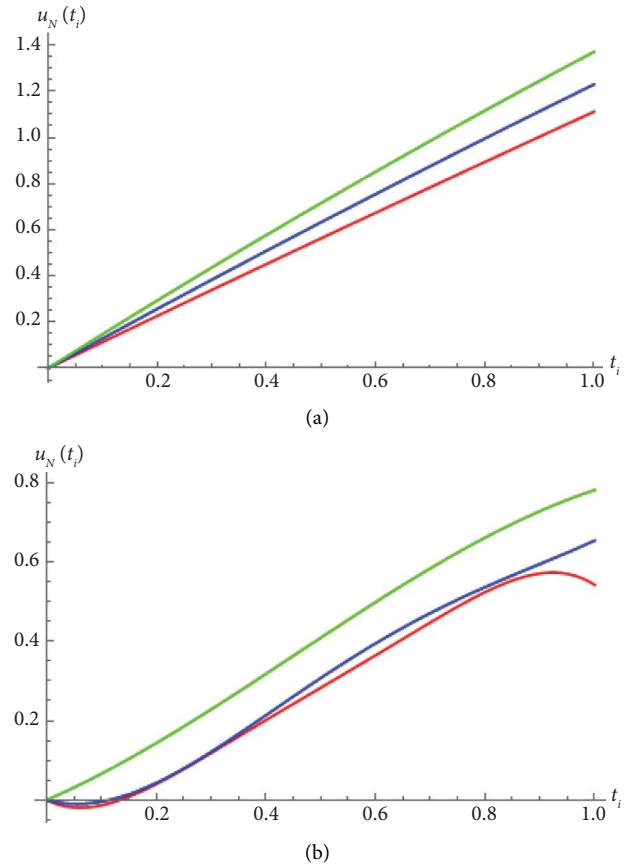

Figure 5: Schematic effects in Example 2 as (a) $\mathbb{U}_N(\mathbb{T})$ at $\varkappa \in \{0.65, 0.7, 0.75\}$ and $N = 3$ as red: $\varkappa = 0.75$, blue: $\varkappa = 0.7$, and green: $\varkappa = 0.65$ and (b) $\mathbb{U}_N(\mathbb{T})$ at $N \in \{4, 5, 6\}$ and $\varkappa = 0.75$ as red: $N = 6$, blue: $N = 5$, and green: $N = 4$.

are tabulated. Secondly, in Figure 7,graphical outcomes for $\mathbb{U}_N(\mathbb{T})$ at $\varkappa \in \{0.65, 0.75, 0.85\}$ and $N \in \{4, 5, 6\}$ are sketched.

For Example 5, the subsequence results have been obtained by employing Algorithm 1. Firstly, in Table 6, data outcomes for $\mathbb{U}_N(\mathbb{T})$ at $\varkappa \in \{0.8, 0.85, 0.9, 0.95\}$ and $N = 5$ are tabulated. Secondly, in Figure 8, graphical outcomes for $\mathbb{U}_N(\mathbb{T})$ at $\varkappa \in \{0.7, 0.8, 0.9\}$ and $N \in \{3, 4, 5\}$ are sketched.

Figures 1 and 2 indicate the accuracy and capacity of the presented algorithm. It should be noted that a few terms of SLPs produce approximate solutions with few errors. Other figures show that the approximate paths of the exact stochastic process paths for example with stochastic terms are smooth. This could be explained by the algorithm of approximation used to obtain these approximations which are mentioned in Section 4.

Table 4: Comparison of results using $\mathbb{U}_N(\mathbb{T}_i)$ at $\varkappa \in \{0.7, 0.75, 0.8, 0.85\}$ and $N = 5$ in Example 3.

$(t_i, \varkappa)$	$\varkappa = 0.7$	$\varkappa = 0.75$	$\varkappa = 0.8$	$\varkappa = 0.85$
0.1	−0.0004127422014683	−0.0002893298202559	−0.0001833975053145	−0.0000941391090036
0.2	0.0000588410453159	0.0001523697223739	0.0002314091041949	0.0002961616403482
0.3	0.0026590907230018	0.0025643610196801	0.0024698905950957	0.0023746548012071
0.4	0.0088540711570229	0.0084238006979336	0.0080133227925925	0.0076203429226518
0.5	0.0203315700155966	0.0194457396178854	0.0185987865805265	0.0177874785496877
0.6	0.0390010983097246	0.0375831228747671	0.0362191679013761	0.0349055642232469
0.7	0.0669938903931927	0.0650267897982904	0.0631231577562564	0.0612793524801887
0.8	0.1066629039625707	0.1042054739526474	0.1018152522049194	0.0994888458532991
0.9	0.1605828200572126	0.1577858031365103	0.1550557523657540	0.1523892968712907
1	0.2315500430592565	0.2286722993830319	0.2258607644157859	0.2231112080588032

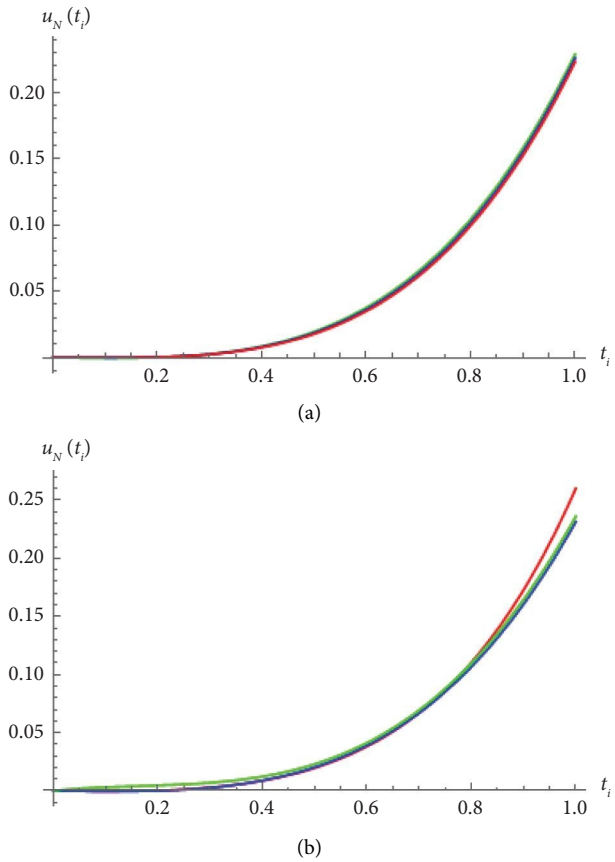

Figure 6: Schematic effects in Example 3 as (a) $\mathbb{U}_N(\mathbb{T})$ at $\varkappa \in \{0.75, 0.80, 0.85\}$ and $N = 5$ as red: $\varkappa = 0.85$, blue: $\varkappa = 0.8$, and green: $\varkappa = 0.7$ and (b) $\mathbb{U}_N(\mathbb{T})$ at $N \in \{4, 5, 6\}$ and $\varkappa = 0.7$ as red: $N = 6$, blue: $N = 5$, and green: $N = 4$.

Table 5: Comparison of results using $\mathbb{U}_N(\mathbb{T}_i)$ at $\varkappa \in \{0.65, 0.7, 0.75, 0.8\}$ and $N = 6$ in Example 4.

$(\mathbb{T}_i, \varkappa)$	0.65	0.7	0.75	0.8
0.1	0.3913120126338804	0.4206886848222444	0.4513106061439101	0.4831487366853607
0.2	0.5383037560425622	0.5707857541545684	0.6043460490239569	0.6389626317093883
0.3	0.6637390345086291	0.6953635664701379	0.7277267653406052	0.7608144058867365
0.4	0.8494176853980600	0.8833143172436895	0.9177895666794504	0.9528279878374484
0.5	1.1094806426628994	1.1481059762731416	1.1872014054867233	1.2267436303981336
0.6	1.4637150003439157	1.5085382250011872	1.5535731410447830	1.5987830270331393
0.7	2.0108590760732756	2.0694983938369040	2.1280733054476180	2.1865144282457223
0.8	3.0019074745772160	3.1027173994773527	3.2040418695763540	3.3057177579892176
0.9	4.9134161511787010	5.1275256822292050	5.3456040090747760	5.5672497300782450
1	8.5208074753000850	8.9916091433302940	9.4762838703247280	9.9739089645998360

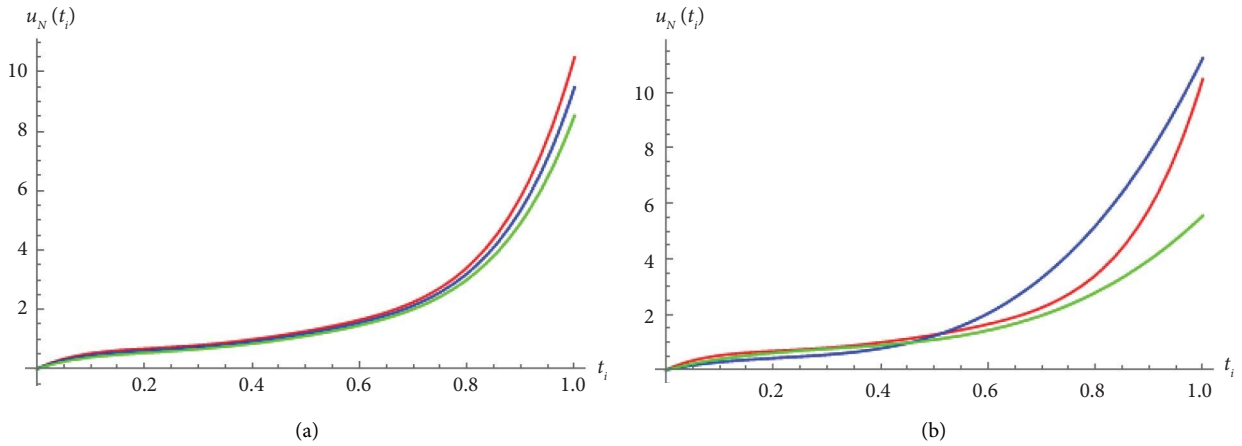

FIGURE 7: Schematic effects in Example 4: (a)$\mathbb{U}_N(\mathbb{T})$ at $\varkappa \in \{0.65, 0.75, 0.85\}$ and $N = 6$ as red: $\varkappa = 0.85$, blue: $\varkappa = 0.875$, and green: $\varkappa = 0.65$ and (b) $\mathbb{U}_N(\mathbb{T})$ at $N \in \{4, 5, 6\}$ and $\varkappa = 0.85$ as red: $N = 6$, blue: $N = 5$, and green: $N = 4$.

TABLE 6: Comparison of results using $u_N(t_i)$ at $\varkappa \in \{0.8, 0.85, 0.9, 0.95\}$ and $N = 5$ in Example 5.

$(\mathbb{T}_i, \varkappa)$	0.8	0.85	0.9	0.95
0.1	0.0328350115386641	0.0319755079774259	0.0311641353015908	0.0336802406189057
0.2	0.0468490515782034	0.0451694310893953	0.0436047631363799	0.0448770698755013
0.3	0.0610566935063954	0.0582384052692908	0.0556195145982813	0.0536871650666798
0.4	0.0894638365572117	0.0849763946447150	0.0807878627856139	0.0749849237398233
0.5	0.1410677058108186	0.1343146915374900	0.1279711228011017	0.1184224636928027
0.6	0.2198568521935767	0.2103219164636579	0.2013124517518740	0.1884296229739785
0.7	0.3248111524780408	0.3122040181334811	0.3002368487494643	0.2842139598822000
0.8	0.4499018092829604	0.4343042734514413	0.4194511549098121	0.3997607529668055
0.9	0.5840913510732793	0.5661032875162400	0.5489440533532615	0.5238330010276226
1	0.7113336321601353	0.6922189936207985	0.6739860692045610	0.6399714231149685

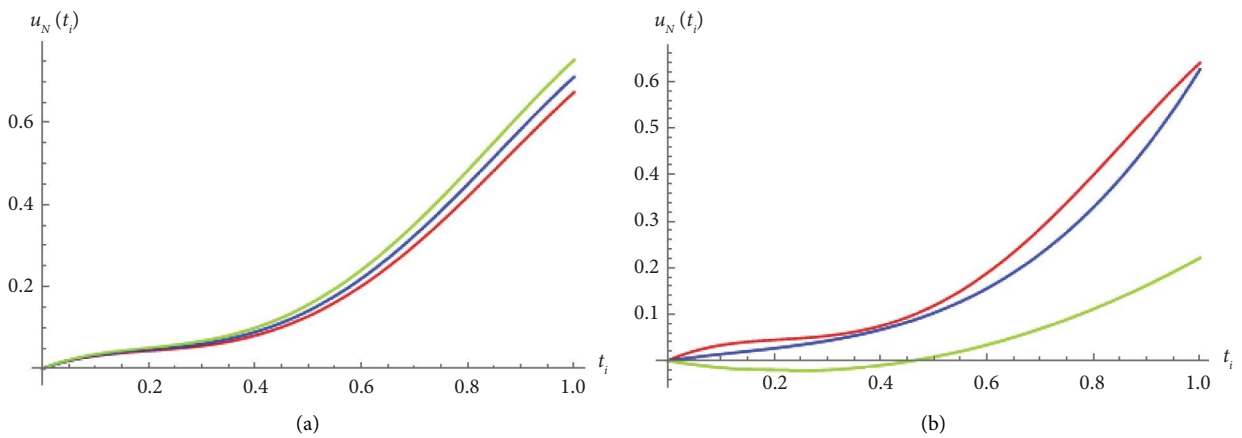

FIGURE 8: Graphical results in Example 5: (a) $\mathbb{U}_N(\mathbb{T})$ at $\varkappa \in \{0.7, 0.8, 0.9\}$ and $N = 5$ as red: $\varkappa = 0.9$, blue: $\varkappa = 0.8$, and green: $\varkappa = 0.7$ and (b) $\mathbb{U}_N(\mathbb{T})$ at $N \in \{3, 4, 5\}$ and $\varkappa = 0.95$ as red: $N = 5$, blue: $N = 4$, and green: $N = 3$.

6. Conclusions and Future Works

This work is mainly proposed to prove and confirm the uniqueness and existence of the suggested solution of a particular form of fractional SIDEs and construct a straightforward, simple, and effective numerical algorithm that provides approximate solutions to complicated problems modeling real-world phenomena. For the theoretical part, the Picard iteration criterion with some topological theorems has been applied to the integral form of (1). For achieving the numerical aim, we have introduced the SLPs and employed them as base functions for a spectral collocation method to have the so-called SL-SCA. The Itô's integral in (1) has been approximated using a well-known numerical integration method and the values of the SBM have been approximated via an effective method. Also, the

convergence analysis of the proposed algorithm has been discussed. Moreover, using the algorithm given in Section 5, three linear and two nonlinear examples of fractional SIDEs have been successfully solved. The outcomes assert that the SL-SCA is a powerful and convenient method. Accurate approximations can be achieved via a few terms of SLPs. For upcoming research, this algorithm is suggested to be employed for solving fractional SIDEs with fractional stochastic SBM of order $H \in (0, 1)$.

Abbreviations

SDE: Stochastic differential equation
SIDE: Stochastic integrodifferential equation
FDE: Fractional differential equation
SLP: Shifted Legendre polynomial
CFD: Conformable fractional derivative
SBM: Standard Brownian motion
SL-SCA: Shifted Legendre spectral collocation algorithm
WP1: With probability one
CSI: Cauchy–Schwartz inequality.

Data Availability

The datasets used for generating the plots and results during the current study are available in the numerical simulation of the related mathematical equations within the article.

Conflicts of Interest

The authors declare that they have no conflicts of interest.

References

[1] J. Hadamarad, "Essai sur l'etude des fonctions donnees par leur developpment de Taylor, Journal de mathématiques pures et appliquées," *Journal de Mathematiques Pures et Appliquees*, vol. 4, pp. 101–186, 1892.

[2] R. Khalil, M. Al Horrani, A. Yousef, and M. Sababheh, "A new definition of fractional derivative," *Journal of Computational and Applied Mathematics*, vol. 264, pp. 65–70, 2014.

[3] M. Caputo and M. Fabrizio, "A new definition of fractional derivative without singular kernel," *Progress in Fractional Differentiation and Applications*, vol. 1, pp. 73–85, 2015.

[4] A. Atangana and D. Baleanu, "New fractional derivatives with non-local and non-singular kernel: theory and application to heat transfer model," *Thermal Science*, vol. 20, no. 2, pp. 763–769, 2016.

[5] E. Ahmed, A. Hashish, and F. A. Rihan, "On fractional order cancer model," *Journal of Fractional Calculus and Applied Analysis*, vol. 3, pp. 1–6, 2012.

[6] F. A. Rihan, "Numerical Modeling of Fractional-Order Biological System," *Abstract and Applied Analysis 2013*, vol. 2013, Article ID 816803, 2013).

[7] H. Xu, "Analytical approximations for a population growth model with fractional order," *Communications in Nonlinear Science and Numerical Simulation*, vol. 14, no. 5, pp. 1978–1983, 2009.

[8] L. Debnath, "Recent applications of fractional calculus to science and engineering," *International Journal of Mathematics and Mathematical Sciences*, vol. 2003, no. 54, pp. 3413–3442, 2003.

[9] N. Sweilam, "Fourth order integro-differential equations using variational iteration method," *Computers & Mathematics with Applications*, vol. 54, no. 7-8, pp. 1086–1091, 2007.

[10] A. Arikoglu and I. Ozkol, "Solution of fractional integro-differential equations by using fractional differential transform method," *Chaos, Solitons & Fractals*, vol. 40, no. 2, pp. 521–529, 2009.

[11] S. Sharma, R. K. Pandey, and K. Kumar, "Collocation method with convergence for generalized fractional integro-differential equations," *Journal of Computational and Applied Mathematics*, vol. 342, pp. 419–430, 2018.

[12] F. Sultana, D. Singh, R. K. Pandey, and D. Zeidan, "Numerical schemes for a class of tempered fractional integro-differential equations," *Applied Numerical Mathematics*, vol. 157, pp. 110–134, 2020.

[13] J. R. Loh, C. Phang, and K. G. Tay, "New method for solving fractional partial integro-differential equations by combination of Laplace transform and resolvent kernel method," *Chinese Journal of Physics*, vol. 67, pp. 666–680, 2020.

[14] N. T. Dung, "Fractional stochastic differential equations with applications to finance," *Journal of Mathematical Analysis and Applications*, vol. 397, no. 1, pp. 334–348, 2013.

[15] L. D. S. Lima, "Fractional stochastic differential equation approach for spreading of diseases," *Entropy*, vol. 24, no. 5, p. 719, 2022.

[16] M. Han, Y. Xu, and B. Pei, "Mixed stochastic differential equations: averaging principle result," *Applied Mathematics Letters*, vol. 112, Article ID 106705, 2021.

[17] B. Pei, y. Xu, and j. l. Wu, "Stochastic averaging for stochastic differential equations driven by fractional Brownian motion and standard Brownian motion," *Applied Mathematics Letters*, vol. 100, Article ID 106006, 2020.

[18] Z. Guo, J. Hu, and W. Wang, "Caratheodory's approximation for a type of Caputo fractional stochastic differential equations," *Advances in Difference Equations*, vol. 2020, no. 1, p. 636, 2020.

[19] X. Zhang, P. Chen, A. Abdelmonem, and Y. Li, "Fractional stochastic evolution equations with nonlocal initial conditions and noncompact semigroups," *Stochastics*, vol. 90, no. 7, pp. 1005–1022, 2018.

[20] S. Moualkia and Y. Xu, "On the existence and uniqueness of solutions for multidimensional fractional stochastic differential equations with variable order," *Mathematics*, vol. 9, no. 17, p. 2106, 2021.

[21] X. Zheng, Z. Zhang, and H. Wang, "Analysis of a nonlinear variable-order fractional stochastic differential equation," *Applied Mathematics Letters*, vol. 107, Article ID 106461, 2020.

[22] A. Ahmaadov and N. Mahmud, "Existence and uniqueness results for a class of fractional stochastic neutral differential equations, Chaos," *Solitons & Fractals*, vol. 139, Article ID 110253, 2020.

[23] M. Khodabin, K. Maleknejad, and T. Damercheli, "Approximate solution of the stochastic Volterra integral equations via expansion method," *International Journal of Industrial Mathematics*, vol. 6, pp. 41–48, 2014.

[24] M. Kamrani, "Numerical solution of stochastic fractional differential equations," *Numerical Algorithms*, vol. 68, no. 1, pp. 81–93, 2014.

[25] S. Kouhkani, H. Koppelaar, and R. Pettersson, "Numerical solution of fractional Stochastic integro-differential equations by the operational Tau method," *International Journal of Statistical Analysis*, vol. 1, pp. 1–9, 2019.

[26] F. Mohammadi, "A Chebyshev wavelet operational method for solving stochastic Volterra-Fredholm integral equations,"

International Journal of Applied Mathematical Research, vol. 4, no. 2, pp. 217–227, 2015.

[27] A. Cardone, R. D'Ambrosio, and B. Paternoster, "A spectral method for stochastic fractional differential equations," *Applied Numerical Mathematics*, vol. 139, pp. 115–119, 2019.

[28] F. Mirzaee and S. F. Hoseini, "Numerical approach for solving nonlinear stochastic Ito-Volterra integral equations using Fibonacci operational matrices," *Scientia Iranica D*, vol. 22, pp. 2472–2481, 2015.

[29] M. Asgari, E. Hashemizadeh, M. Khodabin, and K. Maleknejad, "Numerical solution of nonlinear stochastic integral equation by stochastic operational matrix based on Bernstein polynomials," *Bulletin mathématique de la Société des Sciences Mathématiques de Roumanie*, vol. 1, pp. 3–12, 2014.

[30] Z. Taheri, S. Javadi, and E. Babolian, "Numerical solution of stochastic fractional integrodifferential equation by the spectral collocation method," *Journal of Computational and Applied Mathematics*, vol. 321, pp. 336–347, 2017.

[31] C. Huang and Z. Zhang, "The spectral collocation method for stochastic differential equations," *Discrete & Continuous Dynamical Systems - B*, vol. 18, no. 3, pp. 667–679, 2013.

[32] Y. Wang, "A stochastic Fubini theorem: BSDE method," *Journal of Inequalities and Applications*, vol. 2017, no. 1, p. 77, 2017.

[33] X. Wang and S. Fan, "A class of stochastic Gronwall's inequality and its application," *Journal of Inequalities and Applications*, vol. 2018, no. 1, p. 336, 2018.

[34] Y. V. Prokhorov, "Convergence of random processes and limit theorems in probability theory," *Theory of Probability and Its Applications*, vol. 1, no. 2, pp. 157–214, 1956.

[35] P. Billingsley, *Weak Convergence of Measures: Application in Probability, CBMS-NSF Regional Conference Series in Applied Mathematics*, SIAM, Philadelphia, PS, USA, 1971.

[36] E. Hesameddini and M. Shahbazi, "Legendre collocation method and its convergence analysis for the numerical solutions of the conductor-like screening model for real solvents integral equation," *Bulletin of Computational Applied Mathematics*, vol. 5, pp. 33–51, 2017.

[37] K. M. Saad, "New fractional derivative with non-singular kernel for deriving Legendre spectral collocation method," *Alexandria Engineering Journal*, vol. 59, no. 4, pp. 1909–1917, 2020.

[38] A. H. Bhrawy, L. M. Assas, E. Tohidi, and M. A. Alghamdi, "A Legendre-Gauss collocation method for neutral functional-differential equations with proportional delays," *Advances in Difference Equations*, vol. 2013, no. 1, p. 63, 2013.